Arabian Journal of Chemistry (2023) **16**, 105044

King Saud University

Arabian Journal of Chemistry

www.ksu.edu.sa
www.sciencedirect.com

ORIGINAL ARTICLE

The root essential oil from the Tunisian endemic plant *Ferula tunetana*: Chemical composition, biological evaluation, molecular docking analysis and drug-likeness prediction

Wiem Baccari [a], Ilyes Saidi [a], Insaf Filali [b,*], Mansour Znati [a], Moncef Tounsi [c], Roberta Ascrizzi [d], Guido Flamini [d,e], Hichem Ben Jannet [a,*]

[a] *University of Monastir, Faculty of Science of Monastir, Laboratory of Heterocyclic Chemistry, Natural Products and Reactivity (LR11ES39), Team: Medicinal Chemistry and Natural Products, Avenue of Environment, 5019 Monastir, Tunisia*
[b] *Department of Chemistry, College of Science and Humanities in Al-Kharj, Prince Sattam bin Abdulaziz University, Al-Kharj 11942, Saudi Arabia*
[c] *Preparatory Year Deanship, Basic Science Department, Prince Sattam Bin Abdulaziz University, Alkharj 11942, Saudi Arabia*
[d] *Dipartimento di Farmacia, Università di Pisa, Via Bonanno 6, 56126 Pisa, Italy*
[e] *Centro Interdipartimentale di Ricerca "Nutraceutica e Alimentazione per la Salute" Nutrafood, Via del Borghetto 80, 56124 Pisa, Italy*

Received 29 January 2023; accepted 31 May 2023
Available online 7 June 2023

KEYWORDS

Ferula tunetana;
Root essential oil;
Sesquiterpenes;
Bioactivities;
Molecular docking;
Drug-likeness prediction

Abstract Oxidative stress is closely related to cancer aspects, such as the induction of gene mutations resulting from cellular injury and the effects on transcription and signal transduction factors. In addition, antibiotic resistance is also linked with oxidative stress, which could contribute to the selection of resistant bacterial strains. With this in mind, and considering that essential oils are well known to display antioxidant, antimicrobial, and cytotoxic activities, this study was destined to investigate the chemical composition and to screen these properties for the root essential oil (REO) of the Tunisian endemic species *Ferula tunetana* Pomel ex Batt. The REO GC/MS analysis led to the identification of nine compounds, representing 94.5% of the total oil composition. The phytochemical profile of this essential oil (EO) was characterized by the dominance of sesquiterpenes, comprising 11.7% of sesquiterpene hydrocarbons and 82.8% of oxygenated sesquiterpenes. The three major constituents of the EO were caryophyllene oxide (33.9%), α-cyperone (13.9%), and 14-hydroxy-9-

* Corresponding authors.
E-mail addresses: insaf_filali@yahoo.fr (I. Filali), hichem.bjannet@gmail.com (H. Ben Jannet).
Peer review under responsibility of King Saud University.

Production and hosting by Elsevier

https://doi.org/10.1016/j.arabjc.2023.105044

epi-(*E*)-caryophyllene (12.3%). REO showed a good antioxidant potential against DPPH (IC_{50} = 30.13 ± 0.28 µg/mL), $O_2^{\bullet-}$ (IC_{50} = 42.87 ± 0.81 µg/mL) and H_2O_2 (IC_{50} = 48.03 ± 1.21 µg/mL). Additionally, the antimicrobial activity results showed that REO had a strong antibacterial potential against all target microbial strains, including five Gram-negative, six Gram-positive bacteria, and two *Candida* species (MICs = 0.039–0.625 mg/mL). Furthermore, the extracted EO was found to have good cytotoxic properties against five human cell lines *viz*. HT-29, HCT-116, HeLa, A549 and U937, with IC_{50} values ranging from 3.37 ± 0.02 to 46.66 ± 1.22 µg/mL. The main REO constituents were docked to the human DNA topoisomerase IIα enzyme and the *in vitro* cellular toxicities were rationalized. The drug-likeness of the main compounds identified in the studied EO was predicted. Overall, the results of the current study prove that the EO of *F. tunetana* roots has a noteworthy antioxidant potential and represents an interesting candidate to treat infectious diseases and cancer.

1. Introduction

Over the last decades, the issue of natural antioxidants has arisen and acquired increasing attention in food industry, human nutrition, and medicine. Experts in nutritional research have often reported that the damages generated by diseases in which reactive oxygen species (ROS) are implicated can be avoided by incorporation of antioxidant compounds into human diets. Actually, the formation of ROS has often been correlated to prompt DNA damage, lipid peroxidation, and protein carbonylation, leading to a variety of disorders and chronic health diseases, involving cancer, neurological diseases, aging, and cardiovascular disorders (Engwa, 2018). Therefore, increasing efforts have been devoted to the search for new and safe antioxidant agents. In this context, and by dint of their efficiency and low to no side effects as natural substances, investigations on the various phytochemicals of *Ferula* genus acquired a big attention. They are broadly employed as aroma spices in several cuisines all over the world (Sonigra and Meena, 2021) and possess several biological activities, such as antitumor (Abroudi et al., 2020), antioxidant, antimicrobial (Boghrati and Iranshahi, 2019; Daneshniya et al., 2021), cytotoxic (Hosseinzadeh et al., 2020), insecticidal (Baccari et al., 2020; Liu et al., 2020b; Pavela et al., 2020), anti-acetylcholinesterase (Kahraman et al., 2019a), anticoagulant (Akram and Rashid, 2017), relaxant (Tripathi et al., 2019), antidiabetic (Javanshir et al., 2020), antispasmodic (Shahrajabian et al., 2021), and antiproliferative (Tuncay et al., 2019). This genus belongs to the Apiaceae family, which is composed of about 3,700 plants and 455 genera (Zhou et al., 2020). *Ferula* represents the third largest genus of this family. It has a wide distribution all over Asia, especially in Afghanistan, Iran, North India, the Mediterranean region, and far-East. Tunisian flora records only four species for this genus, comprising *F. tingitana* L., *F. lutea* (Poir.) Maire (synonym of *Ferulago lutea* (Poir.) Grande), *F. communis* L., and *F. tunetana* Pomel ex Batt., which is an endemic Tunisian species growing in different areas and climates all over Tunisia. In 2017, Znati et al. described the detailed analysis of the chemical composition of the seed EO of *F. tunetana*, among 18 compounds identified, α-pinene (39.8%) and β-pinene (11.5%) were the two main compounds. Moreover, this EO was tested for its antioxidant, antimicrobial, and antigerminative activities. In addition, its flower EO was mainly composed of α-pinene (14.3%) and it revealed a potent insecticidal effect, and showed a promising potential in guarding the stored cereals from the red flour beetle aggressions (Baccari et al., 2020). On the other hand, for non-volatile extracts, two new sesquiterpene derivatives, as well as eight known compounds; coladonin coladin, umbelliprenin, isosmarcandin, propiophenone, 13-hydroxyfeselol, stigmasterol and β-sitosterol were isolated from the chloroform extract of the roots (Jabrane et al., 2010). The latest publication on this plant reported the phytochemical profile of its leaf and seed extracts, where vanillic, neochlorogenic and chlorogenic acids were the most abundant constituents (Baccari et al., 2023). However, to the best of our knowledge, there are no published reports on the phytochemical characterization and biological evaluation of the EO of *F. tunetana* roots (REO). Thus, in this research, we aim to cover, for the first time, the chemical profile, antioxidant, antibacterial, and cytotoxic potentials of REO. To better recognize the mechanism of action of this obtained complex mixture for the studied activities, we performed the molecular docking analysis for the main identified compounds in the REO composition within the hydrophobic binding site of the etoposide (EVP) of the protein crystal structure of the human DNA topoisomerase IIα enzyme (PDB: 5GWK). On the other hand, the drug-likeness of the main compounds was predicted.

2. Material and methods

2.1. Plant material

The roots of *F. tunetana* were harvested in Kroussia (Sousse, Tunisia) at the end of March 2020. After authentication at the Bioresources: Integrative Biology and Valorization Laboratory, Higher Institute of Biotechnology of Monastir, University of Monastir, Tunisia, by the botanist, Professor Fethia Harzallah-Skhiri, a specimen of the collected sample was stored at the herbarium of the Laboratory of Heterocyclic Chemistry, Natural Products and Reactivity (LR11ES39), Faculty of Sciences of Monastir, Tunisia, with a voucher specimen number FT-20.

2.2. Hydrodistillation of essential oil

The fresh roots (1.5 kg) were divided into small pieces and submitted to hydrodistillation for 180 min on a Clevenger apparatus in a thermostatically controlled heating. The obtained REO was decanted, dried, weighted, and conserved in the dark into a freezer until further uses.

2.3. Gas Chromatography–Mass spectrometry analysis

As reported by Baccari et al. (2020), the hydrodistilled essential oil was diluted to 0.5% in HPLC-grade *n*-hexane and then injected into a GC–MS apparatus. Gas chromatography–electron impact mass spectrometry (GC–EIMS) analyses were performed with a Varian CP-3800 gas chromatograph (Agilent Technologies Inc., Santa Clara, CA, USA) equipped with an Agilent DB-5 capillary column (Agilent Technologies Inc.,

Santa Clara, CA, USA) capillary column (30 m × 0.25 mm; coating thickness 0.25 µm) and a Varian Saturn 2000 ion trap mass detector (Agilent Technologies Inc., Santa Clara, CA, USA). Analytical conditions were as follows: injector and transfer line temperatures 220 and 240 °C, respectively; oven temperature programmed to rise from 60 to 240 °C at 3 °C/min; carrier gas helium at 1 mL/min; injection of 1 µL (0.5% HPLC grade *n*-hexane solution); split ratio 1:25. Acquisition parameters were as follows: full scan; scan range: 30–300 *m*/*z*; scan time: 1.0 sec. The identification of the constituents was based on a comparison of the retention times with those of pure, authentic samples, comparing their linear retention indices relative to the series of *n*-hydrocarbons (C5-C25). Computer matching was also used against commercial (NIST, 2014) and laboratory-developed mass spectra library built up from pure substances and components of commercial essential oils of known composition and MS literature data (Adams, 2007).

2.4. Radical scavenging activity

2.4.1. DPPH radical scavenging capacity

The DPPH (2,2-diphenyl-1-picrylhydrazyl) assay, usually based on a transfer reaction of hydrogen atom, also involves kinetic data, a mechanism of electron transfer has been proposed for the assay (Gulcin, 2020; Ekaette and Saldaña, 2021). Firstly, the quantification of radical scavenging potential of *F. tunetana* root EO was effected with a quick TLC screening technique using a DPPH solution in methanol (0.2%, w/v). The active compounds manifested as yellow marks against purple surrounding, 30 min after the solution spraying (Ibraheim et al., 2012). In a second step, the spectrophotometric method was performed by means of a published assay process, with some amendments (Zardi-Bergaoui et al., 2020); in brief, the REO and the positive controls (synthetic standard antioxidants: BHT, ascorbic acid, and eugenol) were prepared in MeOH to reach a concentration of 5 mg/mL. Six dilutions were performed to get concentrations ranging from 5 to 0.078 mg/mL. 1 mL of the sample was mixed with the same proportion of the newly prepared solution of 80 µg/mL DPPH-MeOH and permitted to rest for 30 min in the dark at 37 °C for any reaction to occur. At 517 nm, absorbances of the samples were recorded. The inhibition percentage of $DPPH^{\bullet}$ was calculated as follows:

$$I\% = [(Abs_0 - - Abs_1)/Abs_0] \times 100$$

Abs_0: control absorbance (comprising all reagents apart from the tested solution) and Abs_1: sample absorbance. All measurements were realized in triplicate and the studied IC_{50} values were cited as means ± SD of the triplicates.

2.4.2. ABTS radical scavenging activity

The 2,2′-azinobis-3-ethylbenzothiazoline-6-sulfonic acid (ABTS) discoloration technique was used to measure the free radical scavenging activity. In fact, the pure ABTS almost has no apparent absorption peak in the visible spectrum between 400 and 800 nm, while $ABTS^{\bullet+}$, its turquoise oxidation product, exhibits three clear absorption bands located at 414, 660, and 734 nm. Accordingly, the antioxidant capacity of any substances can be spectrophotometrically measured at any wavelength of those bands (Jia et al., 2012). ABTS was solvated in water at a 7 mM of concentration. At pH = 7.4, $ABTS^{\bullet+}$ was generated by the addition of $K_2S_2O_8$. The prepared mixture was left in the dark at room temperature up to 12 h before further use (Zardi-Bergaoui et al., 2018). Methanol was used for dilution of this solution in order to adjust the absorbance at 0.706 ± 0.009 units at 734 nm. 1 mL of a newly prepared $ABTS^{\bullet+}$ solution was added to 1 mL of REO-MeOH solution at diverse concentrations, then the absorbance was gauged 10 min following the initial mixing. Using the same formula applied for the DPPH test, the percentage of inhibition was determined. The ascorbic acid, BHT, and eugenol were also tested as reference for comparison, and the assays were conducted in triplicate.

2.4.3. Superoxide anion radical scavenging activity

The superoxide radical scavenging activity of the REO was estimated by the reduction of NBT (nitro blue tetrazolium), as already reported by Fontana et al. (2001), with slight modifications. Superoxide radicals ($O_2^{\bullet-}$) were produced out of specimen which included nitroblue tetrazolium (NBT) (50 µM), phenazine methosulfate (PMS) (15 µM), and nicotinamide adenine dinucleotide (NADH) (73 µM) (Fontana et al., 2001). The non-enzymatic phenazine methosulfate-nicotinamide adenine dinucleotide [PMS/NADH] system interacts to reduce the NBT to a purple formazan and generates $O_2^{\bullet-}$. 500 µL of each three reagents and REO at different concentrations (0.078–5 mg/mL) were incubated for 2 min at room temperature and the absorbance was measured at 560 nm. Ascorbic acid and eugenol were used as positive controls. The Scavenging activity was determined utilizing the formula as in section 2.4.1. The tests were carried out in triplicate.

2.4.4. Hydrogen peroxide assay

The capacity of REO to reduce H_2O_2 was conducted as specified by Ruch et al. (1989). To do this, 43 mM solution of hydrogen peroxide was readily prepared in phosphate buffer (0.1 M, pH = 7.4). Aliquots of REO at different concentrations (0.078–5 mg/mL) were added to a H_2O_2 solution. Using a spectrophotometer, the absorbance of the mixture was recorded after ten minutes at 230 nm; an extra blank sample without hydrogen peroxide was also prepared for background inference. Eugenol was involved as standard substance, and the tests were performed in triplicate.

2.5. Antimicrobial activity

2.5.1. Microbial strains

The *in vitro* antimicrobial capacity of REO was estimated against a panel of bacteria: 6 Gram-positive (*Staphylococcus aureus ATCC25923, S. epidermidis CIP106510, Bacillus subtilis ATCC 6633, B. cereus ATCC 11778, B. cereus ATCC 14579, Micrococcus luteus NCIMB 8166*), 5 Gram-negative (*Escherichia coli ATCC 25922, E. coli ATCC 35218, Salmonella typhimurium ATCC 13311, S. typhimurium LT2 DT104, Pseudomonas aeruginosa ATCC 27853*), and 2 *yeasts* (*Candida albicans ATCC 90028 and C. glabrata ATCC 90030*).

2.5.2. Disc-diffusion assay

The antimicrobial activity was tested conforming to the protocol depicted by Znati et al. (2012). For the present study, on a

tube comprising 9 mL of Sabouraud Chloramphenicol broth (for *Candida*) and *Mueller–Hinton* broth (for bacteria), a loopful of microbes active stocks was reinforced, then incubated for 24 h at 37 °C. The nightlong cultures were employed for the antimicrobial activity of the REO and the optical density was set at 0.5 McFarland turbidity norms with a DENSIMAT. The respective bacterial inoculums were striped over SB or MH agar plates utilizing a sterile swab. First, 6 mm of diameter sterile filter disks were soaked with 10 µL of REO, and then they were positioned on the suitable agar medium. Amphotericin B (20 µg/disc) and Gentamicin (10 µg/disc) served as positive standard references. The containers were incubated for 24 h at 37 °C for microbial races. The antimicrobial potential was estimated by measurement of diameter of the inhibition zones around each of the discs. Tests were performed in triplicate.

2.5.3. Micro-well determination of MIC and MBC

The minimum inhibitory concentration (MIC) was specified as the lowest concentration of samples that inhibits the bacteria development after overnight incubation. In this work, it was determined as described by Chortani et al. (2020), in sterile 96-well plates with final volume of 200 µL in each well. The REO was dissolved in 10% DMSO. A series of varied concentrations were prepared by two-fold dilutions from the highest concentration of 20 mg/mL to 0.078 mg/mL in 5 mL sterile test tubes comprising nutritive broth. Every well contained 5 µL of the inoculum, 95 µL of nutritious broth, and 100 µL aliquot from the stock solutions of the EO. The final well included 195 µL of nutrient broth and 5 µL of the inoculum except the essential oil served as the negative control. After incubation for 24 h at 37 °C, the lowest concentration (topmost dilution) for which there was no improvement of turbidity and without visible microbial growth on agar plate was noted as MBC values. All tests were assessed in triplicate.

2.6. Cytotoxic activity

The cytotoxic activity bioassay of REO was evaluated against five human cancer cell lines: two colorectal (HT-29 and HTC 116), cervical (HeLa), lung (A549) and leukemia (U937) cells. The antiproliferative potential was assessed by application of the method described by Jabrane et al. (2011). The cells used in this study were grown in entire RPMI medium complemented with 10% (v/v) fetal calf serum and antibiotics (penicillin and streptomycin). Culture was carried out in flasks placed in an incubator at 37 °C and maintained in a completely humidified atmosphere.

Cells were seeded at an initial concentration of 6,000 or 10,000 cells per well in 96-well plates and handled with growth medium for one day, so that the cells attached well and adhered, then treated with various concentrations of the tested REO. After 48 h, 20 µL of MTT solution (5 mg/mL in PBS solution) was added to the wells and the mixture was incubated for 4 h. All the mixtures were dissolved in 200 µL DMSO. At 570 nm, the optical density was spectrophotometrically determined. Doxorubicin was used as positive control. The tests were replicated twice and results were represented as IC_{50} (µg/mL) values (concentration inhibiting 50% of cell growth). After plotting the percent inhibition versus the log of concentrations, the linear regression equation of the resulting trend line was displayed to determine the IC_{50} value.

2.7. Molecular docking procedure

The chemical structures of the REO constituents of *F. tunetana* were generated and optimized using the software ACD (3D viewer) (https://www.filefacts.com/acd3d-viewer-freeware-info). The enzymatic crystal structure of the human DNA topoisomerase IIα in complex with etoposide (PDB: 5GWK) was downloaded from the protein data bank (https://www.rcsb.org). Before starting, water molecules and the complexed inhibitor ligand (etoposide) were removed. Then, the polar hydrogens were added to the protein structure. Hence, the grid box in the target enzyme has a spacing of 0.375 Å. The grid box, with dimensions of 40 × 40 × 40 points and centered with the coordinates x: 23.35, y: −38.58, and z: −59.57, was generated based on the etoposide binding position at the DNA topoisomerase IIα (PDB: 5GWK). The molecular docking analysis of the main REO components at the protein-binding site was performed using AutoDock Vina software (Trot and Olson, 2010). Ligand-enzyme interactions were construed with the Biovia Discovery Studio Visualizer (BIOVIA, D. S. (2017)).

2.8. Drug-likeness prediction procedure

Physicochemical properties and Lipinski's "rule of five" parameters of main detected compounds were predicted by the online computational tool ADMETlab 2.0 (https://admetmesh.scbdd.com/). Pharmacokinetic properties and bioavailability scores were estimated using SwissADME online server (https://www.swissadme.ch/). Bioactivity scores were predicted through the online Chemoinformatics tools of Molinspiration software (https://www.molinspiration.com). On the other hand, the toxicity risk prediction of the picked compounds was assessed using the OSIRIS Property Explorer (https://www.organic-chemistry.org/prog/peo/).

2.9. Statistical analysis

Statistical analysis was performed using GraphPad Prism 7.0. Data are presented as the mean ± Standard Deviation (SD). The difference between two groups was evaluated using Student's *t*-test. The difference among three groups was determined by one-way ANOVA with a post hoc analysis (Tukey test).

3. Results and discussion

3.1. Chemical composition

The pale yellow and strong-smelling REO was obtained with a 0.06% (w/w) hydrodistillation yield. The identified constituents, their retention indices, and their relative percentages are illustrated in Table 1. In total, nine volatile compounds were identified, accounting for 94.5% of the total composition. They all belonged to the sesquiterpene chemical class, among which the oxygenated ones (82.8%) dominated the REO composition, while sesquiterpene hydrocarbons were far less repre-

Table 1 Chemical composition of the root essential oil (REO) of *Ferula tunetana* identified by GC/MS.

N°	Compounds	LRI[a]	Composition (%)	Identification
1	β-caryophyllene	1419	9.3	GC–MS, RI
2	β -copaene	1430	1.1	GC–MS, RI
3	α-humulene	1455	1.3	GC–MS, RI
4	caryophyllene oxide	1581	**33.9**	GC–MS, RI
5	humulene epoxide II	1607	6.9	GC–MS, RI
6	*T*-muurolol	1642	8.2	GC–MS, RI
7	α -cadinol	1652	7.6	GC–MS, RI
8	14-hydroxy-9-*epi*-(*E*)-caryophyllene	1665	**12.3**	GC–MS, RI
9	α -cyperone	1753	**13.9**	GC–MS, RI
Sesquiterpene hydrocarbons			11.7	
Oxygenated sesquiterpenes			82.8	
Total identified			94.5	

[a] Linear retention indices calculated on a HP-5 capillary column; bold type indicates components > 10%.

sented (11.7%). *β*-Caryophyllene (1,9.3%) *β*-copaene (**2**) (1.1%), and α-humulene (**3**) (1.3%) were the only sesquiterpene hydrocarbons identified in this essential oil. On the other hand, REO was chiefly composed of caryophyllene oxide (**4**, 33.9%), α-cyperone (**9**, 13.9%), 14-hydroxy-9-*epi*-(*E*)-caryophyllene (**8**, 12.3%), *T*-muurolol (**6**, 8.2%), α-cadinol (**7**, 7.6%) and humulene epoxide II (**5**, 6.9%) (Fig. 1).

It is rather interesting to mention that caryophyllene oxide (**4**) and α-cyperone (**9**), which acquires elevated biological potentials, were detected in higher proportions in the REO of the *F. tunetana*. Caryophyllene oxide (**4**) is a well-known oxygenated sesquiterpene, which has enormous applications in medications, nutrition and cosmetics as a protective. It has also a several pharmacological and biological activities, such as anti-inflammatory, antifungal, analgesic and anti-cholinesterase (Savelev et al., 2003; Chavan et al., 2010; Karakaya et al., 2020; Gyrdymova and Rubtsova, 2021; Jassal et al., 2021; Schofs et al., 2021; Moghrovyan et al., 2022). α-Cyperone (**9**), has been denoted as the main constituent of various essential oils from aromatic plants and acquires diverse pharmacological activities like anti-inflammatory, antifungal and anti-tumor, so it influences a large range of biological pathways implicated in cancer treatment (Huang et al., 2018; Pei et al., 2020; Horn and Vediyappan, 2021). To the best of our knowledge, there is no previous data on the detailed chemical composition of this species root EO. On the contrary, many previous reports regarding the chemical composition of *Ferula* genus root EO of different geographical origins are available. Arjmand and Dastan (2020) reported that camphene (19.05%) and α-pinene (16.9%) were the major compounds of *F. haussknechtii* REO from Iran. In the same region, *δ*-cadinene (18.27%) was the main component of *F. aucheri* (Ahmadi et al., 2020). Another report by Shatar (2005) revealed that guaiol (58.8%) represents the major compound of Mongolian *F. ferulaoides*. Al-Ja'fari et al., 2011 also stated α-pinene as the major component, representing 43.3% of the total composition, in the EO of *F. hermonis* from Jordan. Nevertheless, numerous studies on the *Ferula* genus reported the presence of caryophyllene oxide (**4**), the prevalent compound of our REO, as a remarkable constituent such as in *F. glauca* L. (14.3%) (Maggi et al., 2009), *F. communis* L. (8.0%) (Nguir et al., 2016), *F. vesceritensis* Coss. & Dur. (7.6%) (Labed-Zouad et al., 2015), and *F. szovitsiana* D.C. (4.1%) (Dehghan et al., 2007). However, the variation of the chemical profile is affected by diverse abiotic factors, such the climate, soil nature, luminosity, harvest time, and temperature (Silva et al., 2020; Yakhlef et al., 2020). Moreover, the chemical composition of other organs of *F. tunetana* species has been studied during the last decade in our laboratory. It was observed that the essential oil extracted from the roots of *F. tunetana* (REO) presented a very limited number of constituents compared to the EO of the flowers of the same species studied before in our laboratory. Only five common compounds have been identified (*β*-caryophyllene, α-humulene, caryophyllene oxide, humulene epoxide II, and α-cadinol), with the common predominance of oxygenated sesquiterpenes (Baccari et al., 2020). On the other hand, a different chemical composition was noticed in the seed EO of this species, also previously studied in our laboratory, consisting of a high amount of monoterpene hydrocarbons (77.3%) with α-pinene (39.8%) and *β*-pinene (11.5%) being the main compounds (Znati et al., 2017). This may be due to the fact that various plant organs acquire different enzymes, which adjust the biosynthesis of the secondary metabolites (Tian et al., 2019). Meanwhile, the results of the present work seem to propose that its roots could be considered as a new natural source of sesquiterpenes-rich EO.

3.2. Antioxidant activity

The root EO of *F. tunetana* showed IC_{50} values at various levels against four *in vitro* tests (DPPH, $ABTS^{+}$ radicals, $O_2^{\bullet}$ and H_2O_2 assays). Table 2 presents the results of REO as well as the standards used as reference: ascorbic acid, eugenol, and BHT. As shown, the EO displayed a remarkable potential. The highest effect was seen with DPPH test, it was able to reduce the deep purple hued, stable radical 2,2-diphenyl-1-picrylhydrazyl ($DPPH^{\bullet}$) to the yellow tinted diphenylpicrylhydrazine, with an IC_{50} value of 30.13 ± 0.28 μg/mL, followed by the the superoxide anion assay (IC_{50} = 42.87 ± 0.81 μg/mL). On the other hand, the studied REO reduces H_2O_2 with an IC_{50} value of 48.03 ± 1.21 μg/mL, whereas it reduces $ABTS^{\bullet+}$ with an IC_{50} value of 61.40 ± 1.67 μg/mL. The antioxidant properties were probably related to the chemical

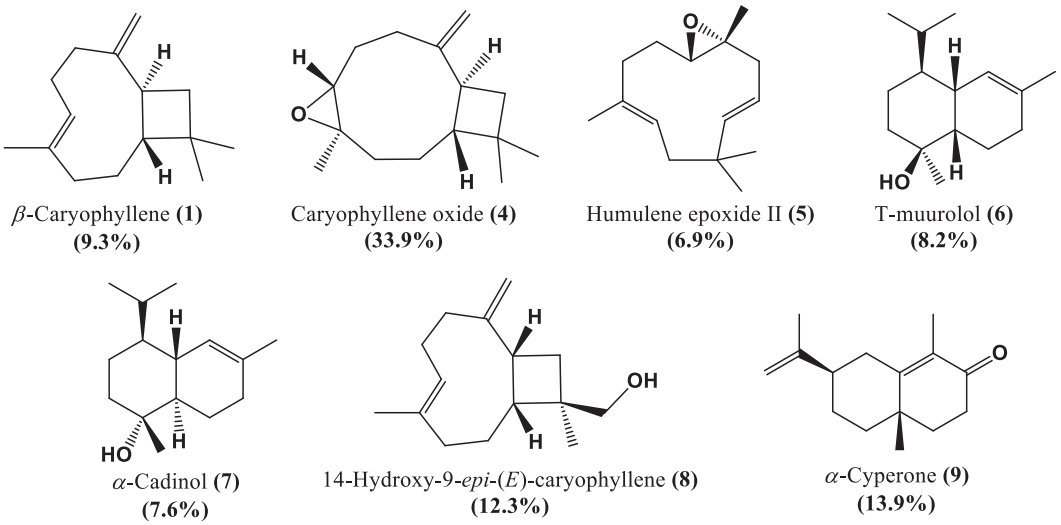

Fig. 1 Chemical structures of the major compounds identified in *Ferula tunetana* root essential oil (REO).

profile, particularly to the high relative percentage of oxygenated sesquiterpenes (82.8%), such as caryophyllene oxide (**4**), α-cyperone (**9**) and 14-hydroxy-9-*epi*-(*E*)-caryophyllene (**8**) (Lemouchi et al., 2017; Abd-ElGawad et al., 2021). More precisely, the obtained antioxidant potency of REO can be assigned chiefly to the presence of caryophyllene oxide in high proportions (Coté et al., 2017; Figueiredo et al., 2019; Nafis et al., 2019; Cascaes et al., 2022). In fact, caryophyllene oxide, the predominant constituent of REO, has formerly been reported as a compound with remarkable antioxidant potential in DPPH assay, displaying an IC_{50} value of 102.5 µg/mL (Wan Salleh et al., 2015; Sarikurkcu et al., 2018). Other less abundant components, such as, α-humulene (**3**) and *β*-copaene (**2**), can also synergistically participate to the reached antioxidative activity (Mischko et al., 2018; Abd-ElGawad et al., 2020). The aforementioned constituents can be the accountable for the predestined antioxidant activity; however, the synergistic effect of other compounds cannot be undervalued, in agreement with that previously stated for numerous other *Ferula* species. Indeed, among many examined natural antioxidants, those originate from *Ferula* species have attracted a quite interest. Firstly, worth noting that the antioxidant potential of EOs is related to the geographic location as well as the species types and the harvesting time (Kavoosi and Rowshan, 2013). Study of Sharopov et al., (2019) on the measure of antioxidant potential of *F. tadshikorum* M. Pimen EO using DPPH, ABTS and FRAP (ferric reducing antioxidant power) tests suggested weak radical scavenging (IC_{50} = 17.8 and 8.2 mg/mL for DPPH and ABTS, respectively), while the FRAP value was 1072.4 µM Fe(II)/mg of the oil sample. Topdas et al. (2020) reported the antioxidant activity of *F. orientalis* L. by means of DPPH and ABTS radical scavenging assays. Results gave IC_{50} values of 50.04 ± 0.12 µg/mL and 80.78 ± 0.10 µg/mL for DPPH and ABTS tests, respectively. The chloroform extract of *F. caspica* M. Bieb. displayed a weak ABTS radical scavenging activity (88.57 ± 1.24 mg Trolox/g extract), compared to the ethyl acetate extract of the same species (268.28 ± 1.84 mg Trolox/g extract) (Kahraman et al., 2019b). In a similar way, the methanol extract of *F. rigidula* Fisch. ex DC. also showed low antioxidant activity in the DPPH radical scavenging capacity (19.91 ± 0.55 mg TE/g extract) compared to the scavenging ABTS radical result which was more potent (49.25 ± 3.34 mg TE/g extract). This radical scavenging effect can be attributed, at least partially, to the presence of phenols and flavonoids in the extracts (Zengin et al., 2020). Although the cited studies report results on the antioxidant capacity of other *Ferula* species, this study can be deemed as the first itemized statement on the evaluation of antioxidant activity of *F. tunetana* root EO. On the contrary, there is a previous report on the antioxidant properties of the EO extracted from the seeds of the same species, which showed a moderate potential against H_2O_2 and $O_2^{\bullet}$ with IC_{50} values of 78.2 ± 2.98 and 89.2 ± 3.82 µg/mL, respectively (Znati et al., 2017).

3.3. Antimicrobial activity

The antimicrobial activity of *F. tunetana* REO was evaluated by the measurement of its IZD (inhibition zone diameter), MIC (minimum inhibitory concentration), and MBC (minimum bactericidal concentration). Gentamicin and Amphotericin B were used as positive controls. As shown in Table 3, the development of the tested Gram-negative bacteria was inhibited by the root EO, with IZD ranging from 14.6 ± 0.5 to 16.7 ± 0.4 mm, with the exception of *P. aeruginosa* ATCC 27853 (8.1 ± 0.0 mm). On the other hand, among the tested bacteria, *S. typhimurium* ATCC 13311 was the most sensitive strain against the REO, with IZD value of 16.7 ± 0.4 mm. However, the Gram-positive bacteria were rather more resistant to the EO, with IZD varying from 12.1 ± 0.2 to 15.9 ± 0.4 mm. In particular, the tested EO was efficient against *B. subtilis* ATCC 6633, *B. cereus* ATCC 14579, *M. luteus* NCIMB 8166, and *S. aureus* ATCC 25923, with IZD values of 15.9 ± 0.4, 15.2 ± 0.2, 15.2 ± 1.8, and 15.2 ± 2.2 mm, respectively. With regard to *Candida yeasts*, the *F. tunetana* REO inhibited the growth of *C. albicans* ATCC 90028 and *C. glabrata* ATCC 90030, with IZD values of 13.8 ± 1.5 mm and 14.8 ± 0.5 mm, respectively.

Based on the scale cited by Radünz et al. (2019) (strong antimicrobial potential: MIC ≤ 0.5 mg/mL; moderate potential:

Table 2 Antioxidant activity of the root essential oil of *Ferula tunetana*.

Sample	IC_{50} ± SD (μg/mL)			
	DPPH	ABTS	$O_2^{\bullet}$	H_2O_2
REO	30.13 ± 0.28[d]	61.40 ± 1.67[c]	42.87 ± 0.81[c]	48.03 ± 1.21[b]
Ascorbic acid [(SR)]	25.70 ± 0.35[c]	20.19 ± 1.04[a]	22.49 ± 1.09[b]	–
Eugenol [(SR)]	16.07 ± 0.69[a]	20.95 ± 0.59[a]	20.14 ± 0.82[a]	21.22 ± 1.12[a]
BHT [(SR)]	18.35 ± 0.31[b]	49.00 ± 1.11[b]	–	–

BHT: butylatedhydroxytoluene; [(SR)] Standard reference; Inhibitory activity as IC_{50} ± SD μg/mL is the sample concentration providing 50% of inhibition. IC_{50} values in the same column followed by the same letter are not significantly different at p-value < 0.05.

0.6 ≤ MIC ≤ 1.5 mg/mL; weak potential: 1.6 mg/mL ≤ MIC), it appears reasonable to presume that the REO exhibited a prominent antimicrobial activity, with MIC values ranging from 0.039 to 0.625 mg/mL. Considering these values, we noticed that *E. coli* ATCC 25922 from the Gram-negative rods and *S. epidermidis* CIP 106510 from the Gram-positive strains were found to be the most sensitive to REO, with the same MIC value (0.039 mg/mL). Afterwards, the MBC determination showed that REO exerted a bactericidal action (MBC/MIC < 4) against all the tested bacteria, with the exception of *S. epidermidis* CIP 106510 and *M. luteus* NCIMB 8166, towards which REO showed only a bacteriostatic efficacy (MBC/MIC > 4), and *C. albicans* ATCC 90028, against which it showed a fungistatic effect. Our results were found to be in agreement with those of Maggi et al. (2009), reporting that *F. glauca* L. leaf EO, a sesquiterpene-rich oil (73.1%), had notable antibacterial activity against *B. subtilis* ATCC 6633, with MIC value of 0.078 mg/mL. It is important to mention that caryophyllene oxide (14.3%) is one of the main constituents of this EO, like the composition of the present study. Another study on the antimicrobial potential of *F. haussknechtii* root EO reported its significant antibacterial activity against *S. aureous*, *S. epidermidis*, and *B. pumilus* (Arjmand and Dastan, 2020). Karakaya et al. (2019), too, reported the importance of caryophyllene oxide and β-caryophyllene in the EO of the aerial parts of *F. orientalis* and *H. microcarpumen* in significant proportions (23.1 and 31.4%, respectively) as antimicrobial agents against *C. albicans* and *S. aureus*, in accordance with the present results. Moreover, according to Coté et al. (2017), caryophyllene oxide separately tested from *Tanacetum vulgare* L. EO was among the main responsible for the antimicrobial activity against *E. coli* (IC_{50} = 97 ± 2 μg/mL) and *S. aureus* (IC_{50} = 10.4 ± 0.9 μg/mL), while the crude EO was less effective against the same two microorganisms with IC_{50} values of 241 ± 13 and 59 ± 5 μg/mL, respectively. Therefore, the antimicrobial activity of REO could be attributed to the high concentration of caryophyllene oxide (33.9%). other studies have shown the importance of β-caryophyllene and its isomer, α-humulene, as antibacterial agents (Sabulal et al., 2006; Ullah et al., 2021). Thus, the presence of β-caryophyllene (9.3%) and α-humulene (1.3%) in REO may also explain the antimicrobial potential against the studied bacteria. Usually, it is difficult to match the antimicrobial potential to a single specific compound because of the great number of compounds constituent the EOs. Nevertheless, the mechanism of cell death has been explained in different studies: the antimicrobial operation was linked to the dissolution of EO compounds in the lipids present in the membrane of microbial cell and mitochondria by dint of their lipophilic nature, which leads to a cell damage by disturbing the cell membrane and causing ionic leakage (Ksouda et al., 2019). Eventually, our results were added to those obtained by Znati et al. (2017), which revealed an interesting antimicrobial activity of *F. tunetana* seed EO rich in monoterpene hydrocarbons (77.3%) against the same bacterial and fungal strains.

3.4. Cytotoxic activity

In this investigation, the cytotoxic activity of the extracted EO was estimated against the human cervical cancer HeLa, human lung cancer A549, human leukemia U937, and human colon cancer HCT-116 and HT-29 cell lines. Results of REO cytotoxicity potential are given in Table 4.

As stated by the American National Cancer Institute, samples with IC_{50} values up to 30 μg/mL against the target cells can be considered as effective anticancer agent for furthermore therapies improvement (Zardi-Bergaoui et al., 2020). The obtained results revealed that REO displayed a significant cytotoxicity against HeLa, A549 and U937 cell lines with IC_{50} values of 3.37 ± 0.02, 8.17 ± 0.29 and 13.82 ± 0.16 μg/mL, respectively, but it was less active towards HT-29 (IC_{50} = 21.13 ± 0.16 μg/mL) and HCT-116 (IC_{50} = 46.66 ± 1.22 μg/mL) colon cells. The HeLa cancer cell line seems particularly sensitive to REO treatments. This finding may be explained by its high caryophyllene oxide (**4**) content (33.9%). Several reports were found regarding the anticancer activities of this compound, as well as its derivatives against various cancer cell lines, including A549, HeLa, HCT-116 and HT-29 cells (Wang et al., 2002; Fidyt et al., 2016; Hanušová et al., 2017; Zardi-Bergaoui et al., 2019; Delgado et al., 2021). Moreover, its distinctive chemical profile is wealthy in natural known anticancer chemical components such as β-caryophyllene (**1**, 9.3%), α-cadinol (**7**, 7.6%), and α-humulene (**3**, 1.3%). It has been reported that these compounds restrained the cell growth of OEC-M1 and A549 cell lines with IC_{50} values varying from 9.9 to 31.3 μg/mL (Su and Ho, 2016). More generally, sesquiterpenes have proven their effectiveness as anticancer agents against human lung A549 and colon DLD-1 cell lines (Sylvestre et al., 2005), and different mechanisms of sesquiterpenes anticancer potential were investigated. Their ability to intensify the oxidative stress in damaged cells is one of them (Ambrož et al., 2019). The actual results are in compliance with those of other researchers who revealed that *Ferula* genus suggests a considerable potency as natural chemotherapeutic agents. The root EO of *F. lutea* showed good cytotoxic potential (IC_{50} = 26.39 ± 3.98 μg/

Table 3 Antimicrobial activity of the root essential oil of *Ferula tunetana*.

Microbial strains	REO			Antibiotics	
	IZD ± SD	MIC	MBC	IZD ± SD	MBC
Bacteria Gram-positive				Gentamicin (SR)	
S. aureus ATCC 25923	15.2 ± 2.2^{e,f}	0.156	0.312	30.6 ± 0.6^{g}	0.726
S. epidermidis CIP 106510	12.1 ± 0.2^{b}	0.039	0.156	20.3 ± 0.5^{a}	1.500
M. luteus NCIMB 8166	15.2 ± 1.8^{e,f}	0.156	0.625	25.6 ± 1.7^{d}	2.250
B. cereus ATCC 11778	12.3 ± 1.2^{b}	0.156	0.156	24.0 ± 0.7^{c}	1.500
B. subtilis ATCC 6633	15.9 ± 0.4^{f,g}	0.078	0.156	29.0 ± 0.4^{f,g}	1.450
B. cereus ATCC 14579	15.2 ± 0.2^{e,f}	0.156	0.156	27.0 ± 1.0^{e}	0.156
Gram-negative					
E. coli ATCC 25922	15.1 ± 0.5^{e}	0.039	0.078	22.0 ± 1.4^{b}	2.250
E. coli ATCC 35218	15.1 ± 1.5^{e}	0.078	0.156	27.7 ± 1.2^{e,f}	0.525
P. aeruginosa ATCC 27853	8.1 ± 0.0^{a}	0.078	0.156	29.3 ± 0.3^{g}	1.270
S. typhimurium ATCC 13311	16.7 ± 0.4^{g}	0.078	0.156	25.3 ± 0.6^{d}	1.275
S. typhimurium LT2 DT104	14.6 ± 0.5^{d}	0.156	0.156	19.0 ± 1.3^{a}	0.650
Candida				Amphotericin B (SR)	
C. albicans ATCC 90028	13.8 ± 1.5^{c}	0.312	1.250	21.2 ± 1.2$^{b'}$	1.900
C. glabrata ATCC 90030	14.8 ± 0.5^{d,e}	0.625	1.250	18.2 ± 0.0$^{a'}$	1.200

IZD ± SD: Inhibition zone diameter (mm) around the discs soaked with 10 µL of essential oil; MBC: Minimum Bactericidal Concentration (mg/mL); MIC: Minimum inhibitory concentration (mg/mL); Gentamicin: (10 µg/disc); Amphotericin B: (20 µg/disc); (SR) Standard reference. IZD values in the same column followed by the same letter are not significantly different at p-value < 0.05.

mL) against the HT-29 cell line (Ben Salem et al., 2016). Likewise, breast MCF7, cervical HeLa and liver HePG2 cell lines were sensitive to *F. tingitana* L. EOs with IC_{50} values ranging from 4.3 and 10.9 µg/mL (Elghwaji et al., 2017).

3.5. Molecular docking studies

DNA topoisomerase enzymes are important enzymes that play essential roles in cellular processes such as transcription, replication, recombination, repair, and catalysis of DNA cleavage. In particular, topoisomerase IIα is preferentially secreted in proliferating cells and considered as the target enzyme for killing cancer cells, on which they depend on this enzyme more than healthy cells, since they divide more rapidly (Lynch et al., 1997; Cowell et al. 2012; Arencibia et al., 2020; Toan et al., 2020). DNA topoisomerase IIα is found in all organisms, from bacteria to human, and even in some viruses (Liu et al. 2018). This enzyme cleaves and relegates DNA to regulate DNA topology and constitutes a major class of antibacterial and anticancer drug targets (Bax et al. 2010). Topoisomerase IIα inhibitors represent a targeted approach to highly proliferative cells and therefore are of particular interest (Lynch et al., 1997; Cowell et al. 2012; Arencibia et al., 2020; Toan et al., 2020). The crystal structure of the human topoisomerase IIα is composed of two chains, A and B, with a sequence length of 806 amino acids (https://www.rcsb.org/structure/5GWK).

Extensive molecular docking studies were executed on the main REO components (**1**, **4**–**9**), to explore the binding mode and rationalize the observed *in vitro* antimicrobial and cytotoxic activities of the EO of *F. tunetana* roots. The structures of the major EO constituents (**1**, **4**–**9**) and etoposide (the standard ligand) were docked within the hydrophobic binding site of the etoposide (EVP) of the protein crystal structure of the human DNA topoisomerase IIα enzyme (PDB: 5GWK) (https://www.rcsb.org/structure/5GWK).

Interestingly, compounds **1**, **4**–**9** behaved as expected. They are perfectly localized in the active pocket of the target enzyme. The binding positions of etoposide (the standard reference) and the major REO components in the structure of the human DNA Topoisomerase IIα enzyme are shown in Fig. 2.

The binding modes of the etoposide and compounds (**1**, **4**–**9**) within the human DNA Topoisomerase IIα enzyme (Fig. 3) are compared below.

The binding mode of the etoposide, the standard inhibitor ligand of the DNA topoisomerase IIα enzyme, showed that it is involved in fifteen non-covalent interactions with seven amino acids. It formed a conventional hydrogen bond with the residue ASP-463, four carbon hydrogen bonds with CD-8, CT-9 and GLY-462, six π-π stacked bonds with DC-8, DT-9 and DG-13, an amide-π stacked binding with ARG-487, an alkyl bond with MET-766 and two π-alkyl bonds with ARG-487 and DT-9 residues (Fig. 3).

The *β*-caryophyllene (**1**) interacted with five amino acids (PRO-439, LYS-440, PHE-484, PRO-485 and ARG-487). The *β*-caryophyllene and the standard ligand, etoposide, share interactions with the residue ARG-487, which indicated that it is in the correct binding pose. It has been implicated just in a π-alkyl and seven alkyl bonds (Fig. 3).

The major compound, caryophyllene oxide (**4**, 33.9%), an oxygenated sesquiterpene, was implicated in eleven non-covalent interactions with five amino acids. Therefore, its binding mode shows that it is properly in the bonding pose and it interacts by three conventional hydrogen bonds with DC-8 and DG-13, four alkyl bonds with ARG-478, and four π-alkyl interactions with DT-9, DA-12 and DG-13 (Fig. 3).

The last five compounds (**5**–**9**) are also oxygenated sesquiterpenes, which constitute a large fraction of the REO (48.9%). Therefore, the molecular insight of docking analysis suggested that all of them exhibited a remarkable conventional hydrogen bond with the residue ASP-463 (Fig. 3). Moreover, the binding mode of humulene epoxide II (**5**), into the target hydrophobic binding site, showed that it is implicated in nine other non-covalent interactions with five residues. Therefore, it formed a π-σ bond with DG-13, three alkyl bonds with

Table 4 Cytotoxic activity of the root essential oil of *Ferula tunetana*.

Samples	IC_{50} ± SD (μg/mL)				
	HT-29	**HCT-116**	**HeLa**	**A549**	**U937**
REO	21.13 ± 0.16[b]	46.66 ± 1.22[b]	3.37 ± 0.02[b]	8.17 ± 0.29[b]	13.82 ± 0.16[b]
Doxorubicin [(SR)]	0.53 ± 0.04[a]	0.63 ± 0.05[a]	1.09 ± 0.06[a]	0.87 ± 0.02[a]	0.29 ± 0.00[a]

[(SR)] Standard reference; Inhibitory activity as IC_{50} ± SD μg/mL is the sample concentration providing 50% of inhibition. IC_{50} values in the same column followed by the same letter are not significantly different at p-value < 0.05.

ARG-487, and five π-alkyl bonds with DC-8, DT-9 and DG-13 (Fig. 3). More of the conventional hydrogen binding with ASP-463, *T*-muurolol **(6)** was involved in three alkyl interactions with the ARG-487 amino acid and eight π-alkyl bonds with DC-8, DA-12, and DG-13. Also, the binding mode of α-cadinol **(7)** showed that it is involved in conventional hydrogen binding with ASP-463, two alkyl bonds with ARG-487 and six π-alkyl bindings with DC-8, DT-9 and DG-13 residues. The molecular insight of docking analysis suggested that, other than the conventional hydrogen binding with ASP-463, 14-hydroxy-9-*epi*-(*E*)-caryophyllene **(8)** interacts with two alkyl bonds with ARG-487 and five π-alkyl bindings with DA-12 and DG-13. The binding analysis suggests that α-cyperone **(9)** forms a conventional hydrogen bond with the ASP-463, a carbon hydrogen bond with GLY-462, two alkyl bonds with ARG-487 and seven π-alkyl bindings with DC-8, DA-12 and DG-13 (Fig. 3).

What is very important is that the conventional hydrogen interaction with ASP-463 is consistent with the single hydrogen bond established by the standard ligand (EVP) with the same residue (ASP-463). The major compound **(4)** interacts in particular *via* three conventional hydrogen bonds, which makes it the most interesting. In addition, the standard ligand (EVP) and the seven docked sesquiterpenes **(1**, **4**–**9)** share an important number of interactions with the two residues ARG-487 and DG-13 (Fig. 3). Therefore, compounds **1**, **4**–**9** are in the perfect bonding position (Figs. 2 and 3). All the aforementioned findings indicate that the binding modes of the docked sesquiterpenes **(1**, **4**–**9)** are very similar to that of the DNA topoisomerase IIα standard inhibitor (EVP) and clearly rationalize the *in vitro* cellular toxicities of the root EO.

3.6. Drug-likeness prediction

3.6.1. Physicochemical properties and Lipinski's "rule of five"

The evaluation of ADMET (Absorption, Distribution, Metabolism, Excretion and Toxicity) properties is considered as key step in drug development processes. Hence, a drug-like product is absorbed within a desired time frame and distributed throughout the body for an efficient metabolism (Bruna et al., 2022). On the other hand, ADMET assessment can be concluded after predicting physicochemical properties and obeying Lipinski's "rule of five" (Ye et al., 2018; Horchani et al., 2022). The physicochemical parameters of a molecular structure, namely molecular weight (MW), molecu-

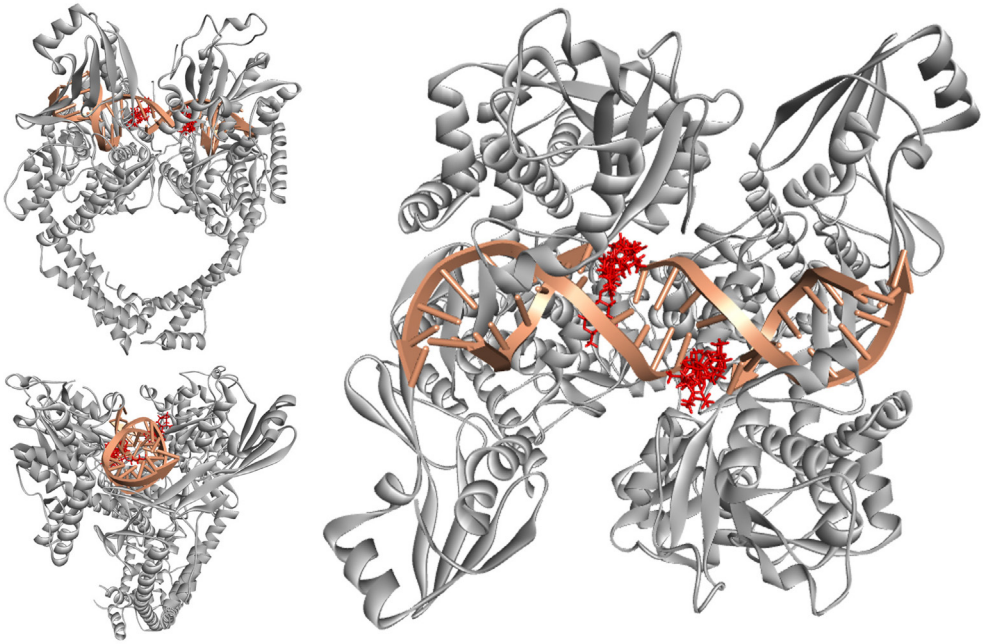

Fig. 2 3D representations of the binding positions of the docked molecules into the hydrophobic binding pocket of EVP in PDB: 5GWK. Compounds **1**, **4**–**9** and Etoposide are indicated by red sticks, double strand DNA is displayed in pink and Topoisomerase IIα enzyme is shown as a grey ribbon.

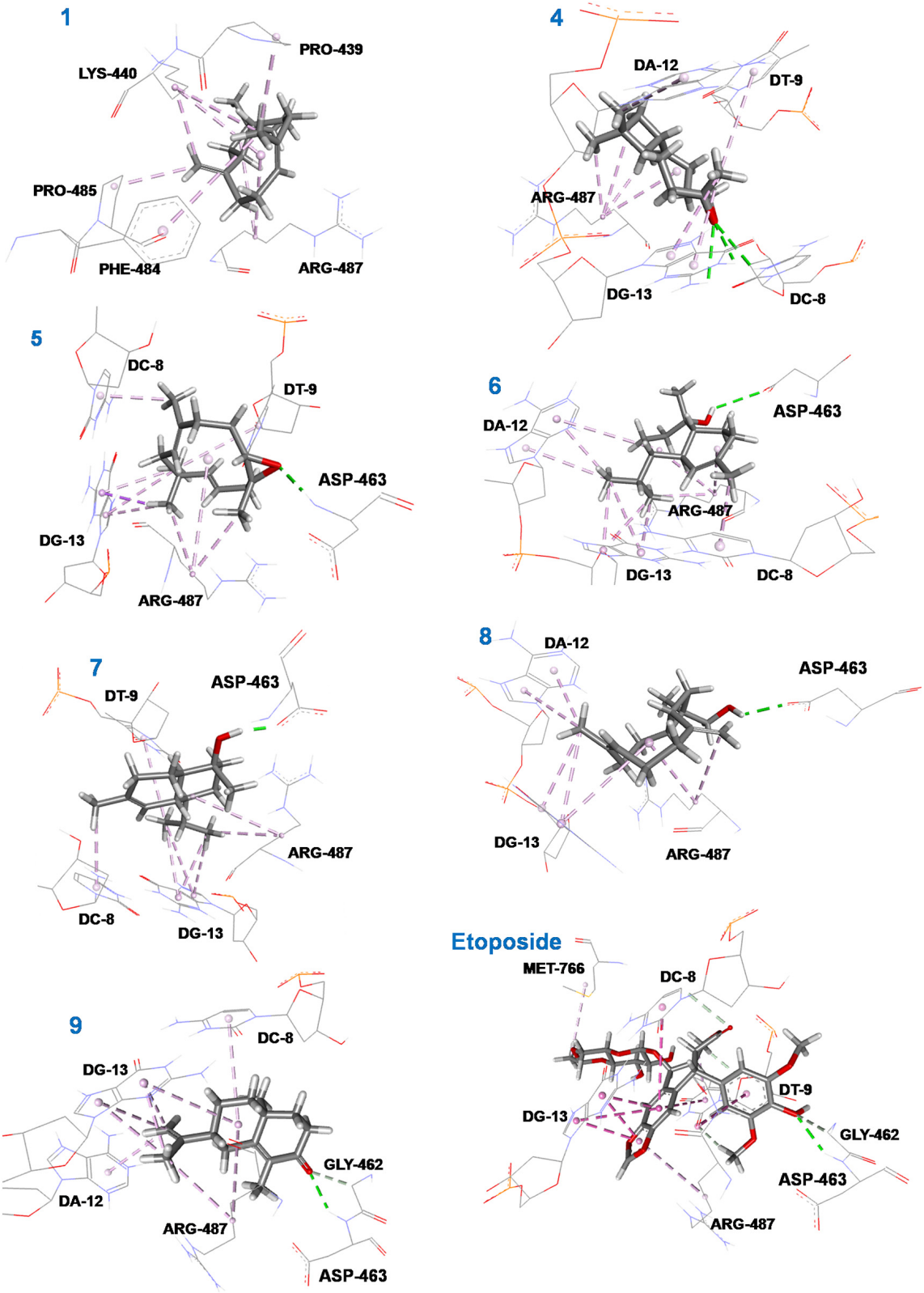

Fig. 3 3D representations of the binding modes of compounds **(1, 4–9)** and etoposide into the hydrophobic binding pocket of EVP in PDB: 5GWK.

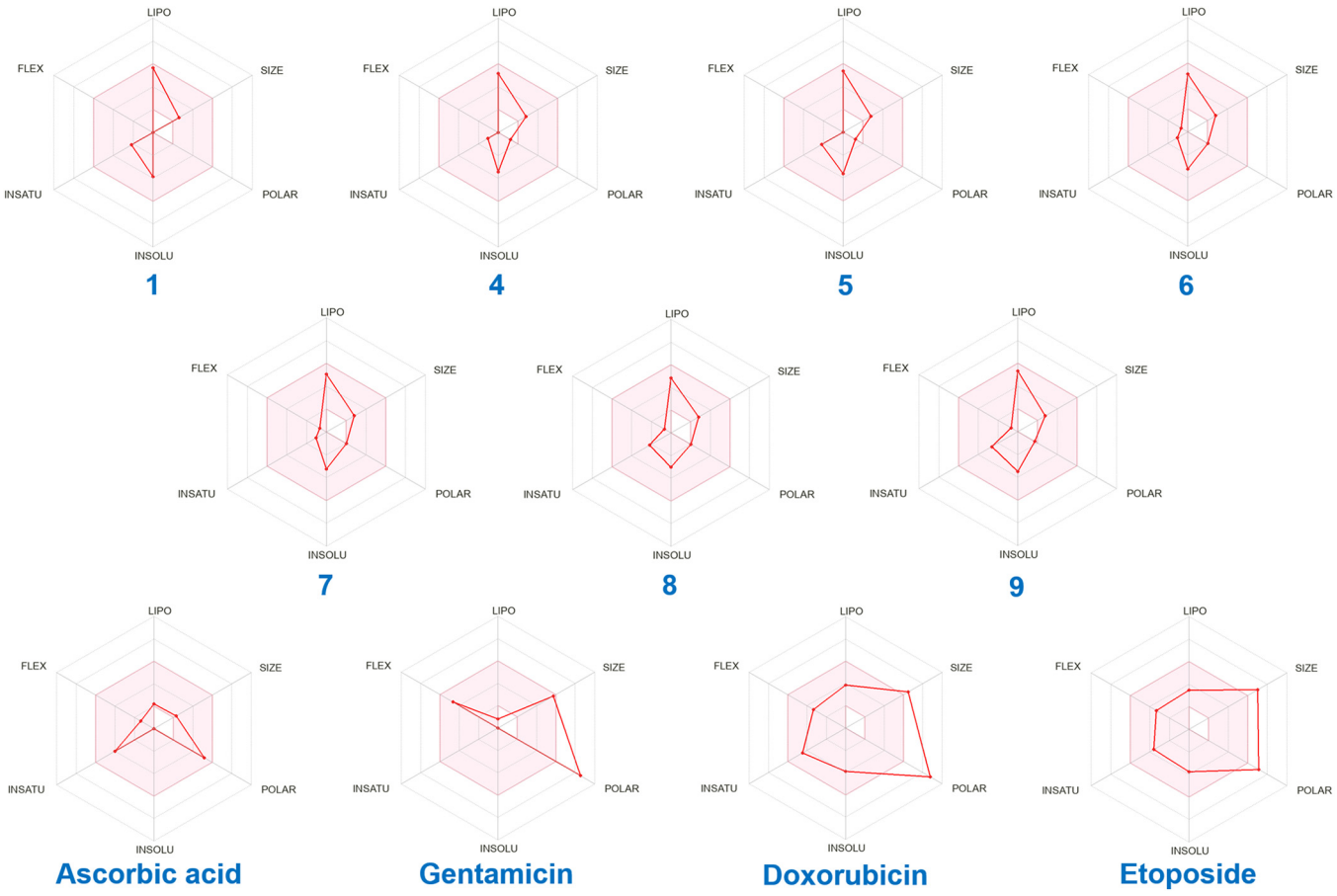

Fig. 4 Bioavailability radar chart of compounds (**1**, **4**–**9**) identified in *Ferula tunetana* root essential oil (REO) and the used standard references. The pink zone is the suitable physicochemical space for oral bioavailability. LIPO (lipophilicity): $-0.7 < \text{XLOGP3} < +5.0$, SIZE: 150 g/mol < MV < 500 g/mol, POLAR (polarity): 20 Å^2 < TPSA < 130 Å^2, INSOLU (insolubility): $-6 <$ Log S (ESOL) < 0, INSATU (insaturation): 0.25 < Fraction Csp^3 < 1, FLEX (flexibility): 0 < Num. rotatable bonds < 9.

Table 5 Predicted Physicochemical Properties and Lipinski Parameters of the major compounds identified in *Ferula tunetana* root essential oil (REO) and the used standard references.

N°	Acceptable value	MW [a]	MV [b]	logS [c]	logP (o/w) [d]	nHA [e]	nHD [f]	nRing [g]	nRB [h]	TPSA [i]	%Abs [j]	nVLip5R [k]
	Compound name	**(100 ~ 600)**	**(500)**	**(-4 ~ 0.5)**	**(0 ~ 3)**	**(≤12)**	**(≤7)**	**(≤6)**	**(≤11)**	**(≤140)**	**(100%)**	**(≤1)**
1	β -caryophyllene	204.190	245.610	−5.810	5.341	0	0	2	0	0.000	109	1
4	caryophyllene oxide	220.180	248.481	−5.296	4.536	1	0	3	0	12.530	104.677	0
5	humulene epoxide II	220.180	254.401	−5.580	4.564	1	0	2	0	12.530	104.677	0
6	*T*-muurolol	222.200	257.037	−3.718	4.723	1	1	2	1	20.230	102.021	0
7	α -cadinol	222.200	257.037	−4.998	4.619	1	1	2	1	20.230	102.021	0
8	14-hydroxy-9-*epi*-(*E*)-caryophyllene	220.180	254.401	−4.064	3.565	1	1	2	1	20.230	102.021	0
9	α -cyperone	218.170	251.764	−4.083	3.929	1	0	2	1	17.070	103.111	0
Ascorbic acid [(SR)]		176.030	151.244	−0.613	−1.420	6	5	1	2	114.290	69.570	0
Gentamicin [(SR)]		477.320	462.618	−0.970	−1.878	12	11	3	7	199.730	40.093	2
Amphotericin B [(SR)]		923.490	932.501	−2.932	−0.249	18	13	3	3	319.610	−1.265	3
Doxorubicin [(SR)]		543.170	516.727	−2.458	2.325	12	7	5	5	212.390	35.725	3
Etoposide [(SR)]		588.180	546.063	−3.573	1.687	13	3	7	5	160.830	53.514	2

[(SR)] Standard reference, [a] Molecular weight, [b] Molecular volume, [c] Log of the aqueous solubility, [d] Log of the octanol/water partition coefficient, [e] Number of hydrogen bond acceptors, [f] Number of hydrogen bond donors, [g] Number of rings, [h] Number of rotatable bonds, [i] Topological polar surface area, [j] Percentage of absorption (%Abs = 109 − [0.345 × TPSA]), [k] Number of violations according to the Lipinski "rule of five".

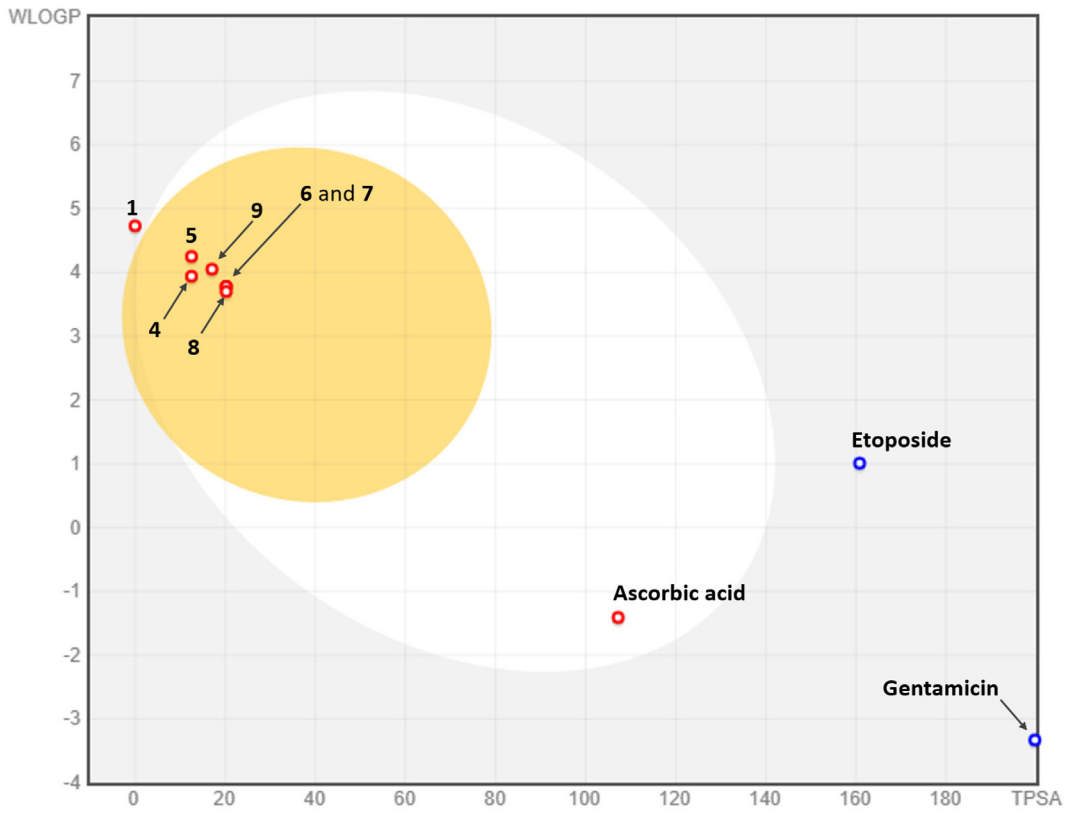

Fig. 5 Boiled-egg graph of compounds (**1**, **4**–**9**) identified in *Ferula tunetana* root essential oil (REO) and the used standard references. Points located in Boiled-Egg's yolk are molecules predicted to passively permeate through the blood–brain barrier. Points located in Boiled-Egg's white are molecules predicted to be passively absorbed by the gastrointestinal tract. Blue dots are for molecules predicted as substrates of P-glycoprotein. In contrast, the red dots correspond to molecules that not predicted to be P-glycoprotein substrates.

Table 6 Predicted Pharmacokinetic Properties and Bioavailability Scores of the major compounds identified in *Ferula tunetana* root essential oil (REO) and the used standard references.

N°	Compound name	GI_a	BBB_p	P-gp_s	$CYP1A2_i$	$CYP2C19_i$	$CYP2C9_i$	$CYP2D6_i$	$CYP3A4_i$	Log K_p	Bioavailability Score
1	β -caryophyllene	Low	No	No	No	Yes	Yes	No	No	−4.44	0.55
4	caryophyllene oxide	High	Yes	No	No	Yes	Yes	No	No	−5.12	0.55
5	humulene epoxide II	High	Yes	No	No	No	Yes	No	No	−4.91	0.55
6	*T*-muurolol	High	Yes	No	No	No	No	No	No	−5.29	0.55
7	α -cadinol	High	Yes	No	No	Yes	No	No	No	−5.29	0.55
8	14-hydroxy-9-*epi*-(*E*)-caryophyllene	High	Yes	No	No	Yes	No	No	No	−5.53	0.55
9	α -cyperone	High	Yes	No	No	Yes	Yes	No	No	−4.93	0.55
Ascorbic acid [(SR)]		High	No	No	No	No	No	No	No	−8.54	0.56
Gentamicin [(SR)]		Low	No	Yes	No	No	No	No	No	−12.12	0.17
Doxorubicin [(SR)]		Low	No	Yes	No	No	No	No	No	−8.71	0.17
Etoposide [(SR)]		Low	No	Yes	No	No	No	Yes	No	−9.46	0.17

[(SR)] Standard reference, GI_a: Gastrointestinal absorption, BBB_p: Blood-brain barrier permeant, P-gp_s: P-glycoprotein substrate, $CYP1A2_i$: Cytochrome P450 1A2 inhibitor, $CYP2C19_i$: Cytochrome P450 2C19 inhibitor, $CYP2C9_i$: Cytochrome P450 2C9 inhibitor, $CYP2D6_i$: Cytochrome P450 2D6 inhibitor, $CYP3A4_i$: Cytochrome P450 3A4 inhibitor, Log *K*p: skin permeation (cm/s).

lar volume (MV), Log of aqueous solubility (logS), Log of octanol/water partition coefficient (logP), number of hydrogen bond acceptors (nHA), number of hydrogen bond donors (nHD), number of rings (nRing), number of rotatable bonds (nRB), topological polar surface area (TPSA), percentage of absorption (%Abs) and number of Violations according to Lipinski's "rule of five" (nVLip5R), are important in predicting the efficacy, the safety, and the drug-likeness properties of a selected compound (Znati et al., 2019; Saidi et al., 2022). Physicochemical parameters and drug-likeness scores

are associated with aqueous solubility, intestinal permeability, oral bioavailability and therefore pharmaceutical properties (Saidi et al., 2022).

The drug-likeness of a selected chemical compound can be predicted with the Lipinski's "rule of five". Lipinski's "rule of five" specifies that most "drug-like" molecules have molecular weight ≤ 500, logP ≤ 5, number of hydrogen bond donors ≤ 5, and number of hydrogen bond acceptors ≤ 10. Indeed, the molecular weight describes the size, the permeability, the transport and the absorption of molecules (https://www.molinspiration.com). LogP value is the best parameter to characterize the molecular hydrophobicity. It is very important in the Quantitative Structure-Activity Relationship (QSAR) study because it is included in the distribution of molecules between fatty and aqueous phases in biological systems (Znati et al., 2019; Saidi et al., 2022). Besides, the ability to give and accept hydrogen bonds indicates the quantification and efficiency of the compound under study to form hydrogen bonds, which improves its interactions and its stability within the active pocket of the target enzyme. Furthermore, bioavailability problems can be reached when more than one of the "rule of five" parameters is violated (https://www.molinspiration.com).

In addition, the analysis of the physicochemical parameters, calculated online with ADMETlab 2.0 (https://admetmesh.scbdd.com/), revealed that all main compounds of the studied REO had scores within the norms and obeyed the Lipinski's "rule of five" (Table 5). As shown in Fig. 4, the bioavailability radar chart, obtained online with SwissADME (https://www.swissadme.ch/), of the major sesquiterpenes identified in REO exhibited significant scores, better than the used standard references. The selected components are entirely in the pink zone, indicating their higher oral bioavailability and drug-likeness. All the predicted sesquiterpenes have molecular weight < 500, therefore, they can be easily absorbed diffused and transported (Znati et al., 2019; Saidi et al., 2022). On the other hand, the octanol/water partition coefficient (logP) of all studied compounds is less than five. Thus, they have a good binding into hydrophobic pocket of enzymes and a best distribution and excretion by metabolism (Saidi et al., 2022). Moreover, all the main components of REO exhibited no violations of the Lipinski's rules, whereas, the used standard references, except for ascorbic acid, violated at least two Lipinski's rules (Table 5 and Fig. 4).

The physicochemical and drug-likeness properties, predicted from the structures of the main compounds of the studied REO, confirm the significant antimicrobial and cytotoxic activities of the tested EO. Therefore, the obtained results suggest that the REO of the *Ferula tunetana* plant may offer therapeutic uses in the future.

3.6.2. Prediction of pharmacokinetic properties

Pharmacokinetic properties are from the best virtual screening filters of bioactive chemical compounds (Bruna et al., 2022; Zafar et al., 2020). To investigate the viability of the major sesquiterpenes (**1**, **4**–**9**) detected in the studied REO, the online tool SwissADME (https://www.swissadme.ch/) was used to predict these pharmacokinetic descriptors. Through the analysis of the Boiled-Egg graph (Fig. 5), it is evident that all oxygenated sesquiterpenes (**4**–**9**), exhibit high gastrointestinal absorption (GI_a) and blood–brain barrier permeability (BBB_p). Since the P-glycoprotein (P-gp) is a membrane protein that removes compounds from cells, it is critical that drug-like compounds are not P-gp substrates. In this respect and according to the estimates made, the tested sesquiterpenes **1**, **4**–**9** fulfilled this condition. The studied compounds (**1**, **4**–**9**) have good skin permeability coefficients (Log *Kp*) from −5.53 to −4.44 (cm/s), which gives them an effective permeability (Liu et al., 2020a; Kirk et al., 2022) to treat skin diseases, better than the used standards. Therefore, and as small hydrophobic chemicals, compounds **4**–**9** have high membrane permeability and they cannot be cleared by P-gp (Bruna et al., 2022).

On the other hand, cytochromes P450 (CYP), also derived from the pharmacokinetic-related proteins, are involved in the oxidative metabolism of compounds, where the oxidized molecules become polar and can thus be excreted, especially by the kidneys within a given time. Noticeably, the studied components interacted with at most two isoenzymes CYP2C19 and CYP2C9 (Table 6), confirming their effectiveness with some secondary toxicities (Alminderej et al., 2020; Bruna et al., 2022). Thus, this finding is consistent with the cellular toxicity

Table 7 Predicted Bioactivity Scores of the major compounds identified in *Ferula tunetana* root essential oil (REO) and the used standard references.

N°	Compound name	GPCR ligand	Ion channel modulator	Kinase inhibitor	Nuclear receptor ligand	Protease inhibitor	Enzyme inhibitor
1	β -caryophyllene	−0.34	0.28	−0.78	0.13	−0.60	0.19
4	caryophyllene oxide	−0.08	0.14	−0.86	0.62	0.00	0.57
5	humulene epoxide II	0.02	−0.19	−0.98	0.79	−0.16	0.80
6	*T*-muurolol	−0.09	0.05	−0.87	0.39	−0.63	0.40
7	α -cadinol	−0.09	0.05	−0.87	0.39	−0.63	0.40
8	14-hydroxy-9-*epi*-(*E*)-caryophyllene	−0.22	0.18	−0.63	0.34	−0.43	0.33
9	α -cyperone	−0.59	−0.27	−1.49	0.22	−0.70	0.12
Ascorbic acid (SR)		−0.53	−0.24	−1.09	−1.01	−0.81	0.20
Gentamicin (SR)		0.34	0.19	0.18	−0.06	0.66	0.46
Amphotericin B (SR)		−3.06	−3.51	−3.54	−3.45	−2.45	−2.95
Doxorubicin (SR)		0.20	−0.20	−0.07	0.32	0.67	0.66
Etoposide (SR)		0.18	−0.48	−0.38	−0.33	0.12	0.30

(SR) Standard reference.

obtained with the *in vitro* assays. Moreover, the bioavailability scores of 0.55 value indicate their more drug-like properties and the high feasibility of use as drugs (Table 6).

3.6.3. Prediction of bioactivity scores

The bioactivity scores of the main compounds identified in the REO of *Ferula tunetana* plant, for biological targets *viz*. G-protein coupled receptor (GPCR) ligand, nuclear receptor ligand, kinase, protease and other enzyme inhibitor, and ion channel modulator based on the online Chemoinformatics tools of Molinspiration software (https://www.molinspiration.com), are showed in Table 7.

In addition, the bioactivity scores of the REO main components can be predicted as active, moderately active or inactive molecules. Precisely, a compound with a positive bioactivity score is predicted to have significant biological activity, while a score value comprise into −0.50 and 0.00, the molecule is expected as moderately active. Nevertheless, the molecule is presumed to be inactive if their score value is less than −0.50 (Znati et al., 2019; Assel et al., 2023).

However, compounds (**1**, **4**, **6**–**9**) were found to have moderate activities as G-protein coupled receptor (GPCR) ligands. Humulene epoxide II (**5**) was predicted with a significant activity. Compounds (**1**, **4**, **6**–**8**) were found to be considerably bioactive as ion channel modulators, and just **5** and **9** were predicted with moderate effects. On the other hand, all the selected compounds were presumed as excellent nuclear receptor ligands and general enzyme inhibitors. For the protease inhibition, just the components **4**, **5** and **8** were found to be moderate inhibitors. Therefore, these computational results supported by the molecular docking analysis validate that the studied REO can be used as natural enzyme inhibitor.

3.6.4. Prediction of toxicity risks

It is primary to determine the toxicity of chemical compounds of medical interest (Srivastava, 2021; Horchani et al., 2022; Assel et al., 2023). Moreover, an *in silico* approach is accessible to estimate certain risks of toxicity *viz*. mutagenicity, tumorigenicity, irritation and reproductive effective (https://www.organic-chemistry.org/prog/peo/). Indeed, with the exception of the medium toxicity risk at the tumorigenicity level estimated for caryophyllene oxide (**4**) and humulene epoxide II (**5**), and at the reproductive effective level predicted for caryophyllene oxide as well, no other toxicity risk was estimated for all other compounds (Table 8).

4. Conclusion

As a contribution in the valorization of the Tunisian endemic flora, this work disclosed for the first time the chemical profile and biological potentials of EO from the roots of *F. tunetana* plant. The results demonstrated that it has a sesquiterpene-chemotype, with 11.7% sesquiterpene hydrocarbons and 82.8% oxygenated sesquiterpenes. Caryophyllene oxide was defined as the major component (33.9%). The REO was found to be a powerful antibacterial mixture against various Gram-positive and Gram-negative bacteria. Furthermore, by means of four complementary assays, the extracted EO showed an important antioxidant activity, especially with DPPH and superoxide anion tests. Results visibly indicated that this EO exhibited cytotoxic potential against human cancer cell lines, *viz*. HeLa, A549, HT-29 and U937 cells. Based on the *in silico* molecular docking analysis, the REO components showed correct binding poses and interesting interactions in the active pocket of the target enzyme DNA topoisomerase IIα, which rationalizes the strong observed *in vitro* cellular toxicity. Overall, these returns, supported by the drug-likeness prediction, proposed that the studied EO could be a promising source of pharmaceuticals.

Funding

This study is supported *via* funding from Prince sattam bin Abdulaziz University project number (PSAU/2023/R/1444).

Declaration of Competing Interest

The authors declare the following financial interests/personal relationships which may be considered as potential competing interests: Insaf FILALI reports financial support, article publishing charges, and equipment, drugs, or supplies were provided by Department of Chemistry, College of Science and Humanities in Al-Kharj, Prince Sattam Bin Abdulaziz University, Alkharj 11942, Saudi Arabia that includes: board membership. Insaf FILALI has patent pending to PSAU/2023/R/1444.

Table 8 Computational Toxicity Risk prediction of the major compounds identified in *Ferula tunetana* root essential oil (REO) and the used standard references.

N°	Compound name	Mutagenicity	Tumorigenicity	Irritation	Reproductive
1	β -caryophyllene	NR	NR	NR	NR
4	caryophyllene oxide	NR	MR	NR	MR
5	humulene epoxide II	NR	MR	NR	NR
6	*T*-muurolol	NR	NR	NR	NR
7	α -cadinol	NR	NR	NR	NR
8	14-hydroxy-9-*epi*-(*E*)-caryophyllene	NR	NR	NR	NR
9	α -cyperone	NR	NR	NR	NR
Ascorbic acid [(SR)]		NR	NR	NR	NR
Gentamicin [(SR)]		NR	NR	NR	NR
Amphotericin B [(SR)]		NR	NR	NR	NR
Doxorubicin [(SR)]		NR	NR	HR	NR
Etoposide [(SR)]		NR	NR	NR	NR

[(SR)] Standard reference, NR: No risk, MR: Medium risk, HR: Higher risk.

Acknowledgement

The authors are grateful to Researchers Supporting Project number (PSAU/2023/R/1444) at Prince sattam bin Abdulaziz University, Saudi Arabia.

Appendix A. Supplementary material

Supplementary data to this article can be found online at https://doi.org/10.1016/j.arabjc.2023.105044.

References

Abd-ElGawad, A.M., Elshamy, A.I., El-Amier, Y.A., El Gendy, A.E. N.G., Al-Barati, S.A., Dar, B.A., Al-Rowaily, S.L., Assaeed, A.M., 2020. Chemical composition variations, allelopathic, and antioxidant activities of *Symphyotrichum squamatum* (Spreng.) Nesom essential oils growing in heterogeneous habitats. Arab. J. Chem. 13, 4237–4245. https://doi.org/10.1016/j.arabjc.2019.07.005.

Abd-ElGawad, A.M., Elgamal, A.M., Ei-Amier, Y.A., Mohamed, T. A., El Gendy, A.E.N.G., Elshamy, I.A., 2021. Chemical composition, allelopathic, antioxidant, and anti-inflammatory activities of sesquiterpenes rich essential oil of *Cleome amblyocarpa* Barratte & Murb. Plants 10 (7), 1294. https://doi.org/10.3390/plants10071294.

Abroudi, M., Fard, A.G., Dadashizadeh, G., Gholami, O., Mahdian, D., 2020. Antiproliferative effects of *Ferula assa-foetida*'s extract on PC12 and MCF7 cancer cells. Int. J. Biomed. Eng. Clin. Sci. 6, 60. https://doi.org/10.11648/j.ijbecs.20200603.12.

Adams, R.P., 2007. Identification of Essential Oil Components by Gas Chromatography/Mass Spectroscopy, 4th ed. allured publishing corporation carol stream, IL, USA.

Ahmadi Koulaei, S., Hadjiakhoondi, A., Delnavazi, M.R., Tofighi, Z., Ajani, Y., Kiashi, F., 2020. Chemical composition and biological activity of *Ferula aucheri* essential oil. Res. J. Pharmacogn. 7, 21–31. https://doi.org/10.22127/rjp.2020.210354.1537.

Akram, M., Rashid, A., 2017. Anti-coagulant activity of plants: mini review. J. Thrombo. Thrombolysis 44, 406–411. https://doi.org/10.1007/s11239-017-1546-5.

Al-Ja'fari, A.H., Vila, R., Freixa, B., Tomi, F., Casanova, J., Costa, J., Cañigueral, S., 2011. Composition and antifungal activity of the essential oil from the rhizome and roots of *Ferula hermonis*. Phytochemistry 72, 1406–1413. https://doi.org/10.1016/j.phytochem.2011.04.013.

Alminderej, F., Bakari, S., Almundarij, T.I., Snoussi, M., Aouadi, K., Kadri, A., 2020. Antioxidant activities of a new chemotype of Piper cubeba L. fruit essential oil (Methyleugenol/Eugenol). In silico molecular docking and ADMET studies. Plants 9, 1534. https://doi.org/10.3390/plants9111534.

Ambrož, M., Šmatová, M., Šadibolová, M., Pospíšilová, E., Hadravská, P., Kašparová, M., Skálová, L., 2019. Sesquiterpenes α-humulene and β-caryophyllene oxide enhance the efficacy of 5-fluorouracil and oxaliplatin in colon cancer cells. Acta Pharm. 69, 121–128. https://doi.org/10.2478/acph-2019-0003.

Arencibia, J.M., Brindani, N., Franco-Ulloa, S., Nigro, M., Kuriappan, J.A., Ottonello, G., Bertozzi, S.M., Summa, M., Girotto, S., Bertorelli, R., Armirotti, A., De Vivo, M., 2020. Design, synthesis, dynamic docking, biochemical characterization, and *in vivo* pharmacokinetics studies of novel topoisomerase II poisons with promising antiproliferative activity. J. Med. Chem. 63, 3508–3521. https://doi.org/10.1021/acs.jmedchem.9b01760.

Arjmand, Z., Dastan, D., 2020. Chemical characterization and biological activity of essential oils from the aerial part and root of *Ferula haussknechtii*. Flavour Fragr. J. 35, 114–123. https://doi.org/10.1002/ffj.3544.

Assel, A., Hajlaoui, A., Lazrag, H., Manachou, M., Romdhane, A., Kraiem, J., Ben Jannet, H., 2023. Synthesis of new sulfamate linked 4-hydroxycoumarin conjugates as potent anti-α-amylase agents: *In vitro* approach coupled with molecular docking, DFT calculation and chemoinformatics prediction. J. Mol. Struct. 1271,. https://doi.org/10.1016/j.molstruc.2022.134020 134020.

Baccari, W., Znati, M., Zardi-Bergaoui, A., Chaieb, I., Flamini, G., Ascrizzi, R., Ben Jannet, H., 2020. Composition and insecticide potential against *Tribolium castaneum* of the fractionated essential oil from the flowers of the Tunisian endemic plant *Ferula tunetana* Pomel ex Batt. Ind. Crops Prod. 143,. https://doi.org/10.1016/j.indcrop.2019.111888 111888.

Baccari, W., Saidi, I., Znati, M., Mustafa, A.M., Caprioli, G., Harrath, A.H., Ben Jannet, H., 2023. HPLC-MS/MS analysis, antioxidant and α-amylase inhibitory activities of the endemic plant *Ferula tunetana* using *in vitro* and *in silico* methods. Process Biochem. 129, 230–240. https://doi.org/10.1016/j.procbio.2023.03.015.

Bax, B.D., Chan, P.F., Eggleston, D.S., Fosberry, A., Gentry, D.R., Gorrec, F., Giordano, I., Hann, M.M., Hennessy, A., Hibbs, M., Huang, J., Jones, E., Jones, J., Brown, K.K., Lewis, C.J., May, E. W., Saunders, M.R., Singh, O., Spitzfaden, C.E., Shen, C., Shillings, A., Theobald, A.J., Wohlkonig, A., Pearson, N.D., Gwynn, M.N., 2010. Type IIA topoisomerase inhibition by a new class of antibacterial agents. Nature 466, 935–940. https://doi.org/10.1038/nature09197.

Ben Salem, S., Znati, M., Jabrane, A., Casanova, J., Ben Jannet, H., 2016. Chemical composition, antimicrobial, anti-acetylcholinesterase and cytotoxic activities of the root essential oil from the Tunisian *Ferula lutea* (Poir.) Maire (Apiaceae). J. Essent. Oil-Bear. Plants 19, 897–906. https://doi.org/10.1080/0972060X.2015.1137238.

Boghrati, Z., Iranshahi, M., 2019. *Ferula* species: a rich source of antimicrobial compounds. J. Herb. Med. 16,. https://doi.org/10.1016/j.hermed.2018.10.009 100244.

Bruna, F., Fernandez, K., Urrejola, F., Touma, J., Navarro, M., Sepúlveda, B., Larrazabal-Fuentes, M., Paredes, A., Neira, I., Ferrando, M., Osorio, M., Yáñez, O., Bravo, J., 2022. Chemical composition, antioxidant, antimicrobial and antiproliferative activity of *Laureliopsis philippiana* essential oil of Chile, study *in vitro* and *in silico*. Arab. J. Chem. 15,. https://doi.org/10.1016/j.arabjc.2022.104271 104271.

Cascaes, M.M., De Moraes, Â.A.B., Cruz, J.N., Franco, C.D.J.P., Silva, E.R.C., Nascimento, L.D.D., Andrade, E.H.D.A., 2022. Phytochemical profile, antioxidant potential and toxicity evaluation of the essential oils from *Duguetia* and *Xylopia* species (Annonaceae) from the Brazilian Amazon. Antioxidants 11 (9), 1709. https://doi.org/10.3390/antiox11091709.

Chavan, M.J., Wakte, P.S., Shinde, D.B., 2010. Analgesic and anti-inflammatory activity of Caryophyllene oxide from *Annona squamosa* L. bark. Phytomedicine 17, 149–151. https://doi.org/10.1016/j.phymed.2009.05.016.

Chortani, S., Edziri, H., Manachou, M., Al-Ghamdi, Y.O., Almalki, S.G., Alqurashi, Y.E., Ben Jannet, H., Romdhane, A., 2020. Novel 1,3,4-oxadiazole linked benzopyrimidinones conjugates: Synthesis, DFT study and antimicrobial evaluation. J. Mol. Struct. 1217,. https://doi.org/10.1016/j.molstruc.2020.128357 128357.

Coté, H., Boucher, M.A., Pichette, A., Legault, J., 2017. Anti-inflammatory, antioxidant, antibiotic, and cytotoxic activities of *Tanacetum vulgare* L. essential oil and its constituents. Medicines 4, 34. https://doi.org/10.3390/medicines4020034.

Cowell, I.G., Sondka, Z., Smith, K., Lee, K.C., Manville, C.M., Sidorczuk-Lesthuruge, M., Rance, H.A., Padget, K., Jackson, G. H., Adachi, N., Austin, C.A., 2012. Model for *MLL* translocations in therapy-related leukemia involving topoisomerase IIβ-mediated DNA strand breaks and gene proximity. Proc. Natl. Acad. Sci. U. S.A. 109, 8989–8994. https://doi.org/10.1073/pnas.1204406109.

Daneshniya, M., Maleki, M.H., Mohammadi, M.A., Ahangarian, K., Kondeskalaei, V.J., Alavi, H., 2021. Antioxidant and antimicrobial activity of *Ferula* Species' essential oils and plant extracts and their

application as the natural food preservatives. J. Asian Nat. Prod. Res. 4, 1–23.

Dehghan, G., Solaimanian, R., Shahverdi, A.R., Amin, G., Abdollahi, M., Shafiee, A., 2007. Chemical composition and antimicrobial activity of essential oil of *Ferula szovitsiana* DC. Flavour Fragr. J. 22, 224–227. https://doi.org/10.1002/ffj.1789.

Delgado, C., Mendez-Callejas, G., Celis, C., 2021. Caryophyllene oxide, the active compound isolated from leaves of *Hymenaea courbaril* L. (Fabaceae) with antiproliferative and apoptotic effects on PC-3 androgen-independent prostate cancer cell line. Molecules 26 (20), 6142. https://doi.org/10.3390/molecules26206142.

Ekaette, I., Saldaña, M.D., 2021. Ultrasound processing of rutin in food-grade solvents: Derivative compounds, antioxidant activities and optical rotation. Food Chem. 344,. https://doi.org/10.1016/j.foodchem.2020.128629 128629.

Elghwaji, W., El-Sayed, A.M., El-Deeb, K.S., ElSayed, A.M., 2017. Chemical composition, antimicrobial and antitumor potentiality of essential oil of *Ferula tingitana* L. Apiaceae grow in Libya. Pharmacogn. Mag. 13, S446. https://doi.org/10.4103/pm.pm_323_15.

Engwa, G.A., 2018. Free Radicals and the Role of Plant Phytochemicals as Antioxidants Against Oxidative Stress-Related Diseases, in Toshiki, A., Asaduzzaman, M.D. (Eds.), Phytochemicals: Source of Antioxidants and Role in Disease Prevention. IntechOpen: London, UK, pp. 49-74. http://dx.doi.org/10.5772/intechopen.76719.

Fidyt, K., Fiedorowicz, A., Strządała, L., Szumny, A., 2016. β-caryophyllene and β-caryophyllene oxide-natural compounds of anticancer and analgesic properties. Cancer Med. 5, 3007–3017. https://doi.org/10.1002/cam4.816.

Figueiredo, P.L.B., Pinto, L.C., da Costa, J.S., da Silva, A.R.C., Mourão, R.H.V., Montenegro, R.C., Maia, J.G.S., 2019. Composition, antioxidant capacity and cytotoxic activity of *Eugenia uniflora* L. chemotype-oils from the Amazon. J. Ethnopharmacol. 232, 30–38. https://doi.org/10.1016/j.jep.2018.12.011.

Fontana, M., Mosca, L., Rosei, M.A., 2001. Interaction of enkephalins with oxyradicals. Biochem. Pharmacol. 61, 1253–1257. https://doi.org/10.1016/S0006-2952(01)00565-2.

Gulcin, İ., 2020. Antioxidants and antioxidant methods: An updated overview. Arch. Toxicol. 94, 651–715. https://doi.org/10.1007/s00204-020-02689-3.

Gyrdymova, Y.V., Rubtsova, S.A., 2021. Caryophyllene and caryophyllene oxide: a variety of chemical transformations and biological activities. Chem. Pap. 76, 1–39. https://doi.org/10.1007/s11696-021-01865-8.

Hanušová, V., Caltová, K., Svobodová, H., Ambrož, M., Skarka, A., Murínová, N., Králová, V., Tomšík, P., Skálová, L., 2017. The effects of β-caryophyllene oxide and *trans*-nerolidol on the efficacy of doxorubicin in breast cancer cells and breast tumor-bearing mice. Biomed. Pharmacother. 95, 828–836. https://doi.org/10.1016/j.biopha.2017.09.008.

Horchani, M., Heise, N.V., Csuk, R., Ben Jannet, H., Harrath, A.H., Romdhane, A., 2022. Synthesis and *in silico* docking study towards M-pro of novel heterocyclic compounds derived from pyrazolopyrimidinone as putative SARS-CoV-2 inhibitors. Molecules 27, 5303. https://doi.org/10.3390/molecules27165303.

Horn, C., Vediyappan, G., 2021. Anticapsular and antifungal activity of α-Cyperone. Antibiotics 10, 51. https://doi.org/10.3390/antibiotics10010051.

Hosseinzadeh, N., Shomali, T., Hosseinzadeh, S., Raouf Fard, F., Jalaei, J., Fazeli, M., 2020. Cytotoxic activity of *Ferula persica* gum essential oil on murine colon carcinoma (CT26) and Vero cell lines. J. Essent. Oil Res. 32, 169–177. https://doi.org/10.1080/10412905.2020.1729880.

Huang, B., He, D., Chen, G., Ran, X., Guo, W., Kan, X., Liu, J., 2018. α-Cyperone inhibits LPS-induced inflammation in BV-2 cells through activation of Akt/Nrf2/HO-1 and suppression of the NF-κB pathway. Food Funct. 9, 2735–2743. https://doi.org/10.1039/C8FO00057C.

Ibraheim, Z.Z., Abdel-Mageed, W.M., Dai, H., Guo, H., Zhang, L., Jaspars, M., 2012. Antimicrobial antioxidant daucane sesquiterpenes from *Ferula hermonis* Boiss. Phytother. Res. 26, 579–586. https://doi.org/10.1002/ptr.3609.

Jabrane, A., Ben Jannet, H., Mighri, Z., Mirjolet, J.F., Duchamp, O., Harzallah-Skhiri, F., Lacaille-Dubois, M.A., 2010. Two new sesquiterpene derivatives from the Tunisian endemic *Ferula tunetana* Pom. Chem. Biodivers. 7 (2), 392–399. https://doi.org/10.1002/cbdv.201600116.

Jabrane, A., Ben Jannet, H., Miyamoto, T., Mirjolet, J.F., Duchamp, O., Harzallah-Skhiri, F., Lacaille-Dubois, M.A., 2011. Spirostane and cholestane glycosides from the bulbs of *Allium nigrum* L. Food Chem. 125, 447–455. https://doi.org/10.1016/j.foodchem.2010.09.028.

Jassal, K., Kaushal, S., Rashmi, Rani, R., 2021. Antifungal potential of guava (*Psidium guajava*) leaves essential oil, major compounds: beta-caryophyllene and caryophyllene oxide. Arch. Phytopathol. Plant Prot. 54(19-20), 2034-2050. Doi: 10.1080/03235408.2021.1968287.

Javanshir, S., Soukhtanloo, M., Jalili-Nik, M., Yazdi, A.J., Amiri, M. S., Ghorbani, A., 2020. Evaluation potential antidiabetic effects of *Ferula latisecta* in Streptozotocin-induced diabetic rats. J. Pharmacopunct. 23, 158–164. https://doi.org/10.3831/KPI.2020.23.3.158.

Jia, S.M., Liu, X.F., Kong, D.M., Shen, H.X., 2012. A simple, post-additional antioxidant capacity assay using adenosine triphosphate-stabilized 2,2′-azinobis(3-ethylbenzothiazoline)-6-sulfonic acid (ABTS) radical cation in a G-quadruplex DNAzyme catalyzed ABTS–H_2O_2 system. Biosens. Bioelectron. 35, 407–412. https://doi.org/10.1016/j.bios.2012.03.029.

Kahraman, C., Baysal, I., Çankaya, I., Goger, F., Kirimer, N., Akdemir, Z.S., 2019a. Acetylcholinesterase inhibitory activities and LC-MS analysis of the antioxidant *Ferula caspica* M. Bieb. and *F. halophila* Pesmen extracts. J. Res. Pharm. 23, 543–551. https://doi.org/10.12991/jrp.2019.161.

Kahraman, C., Topcu, G., Bedir, E., Tatli, I.I., Ekizoglu, M., Akdemir, Z.S., 2019b. Phytochemical screening and evaluation of the antimicrobial and antioxidant activities of *Ferula caspica* M. Bieb. extracts. Saudi Pharm. J. 27, 525–531. https://doi.org/10.1016/j.jsps.2019.01.016.

Karakaya, S., Göger, G., Bostanlik, F.D., Demirci, B., Duman, H., Kilic, C.S., 2019. Comparison of the essential oils of *Ferula orientalis* L., *Ferulago sandrasica* Peşmen and Quézel, and *Hippomarathrum microcarpum* Petrov and their antimicrobial activity. Turk. J. Pharm. Sci. 16, 69–75. https://doi.org/10.4274/tjps.77200.

Karakaya, S., Yilmaz, S.V., Özdemir, Ö., Koca, M., Pınar, N.M., Demirci, B., Baser, K.H.C., 2020. A caryophyllene oxide and other potential anticholinesterase and anticancer agent in *Salvia verticillata* subsp. amasiaca (Freyn & Bornm.) Bornm. (Lamiaceae). J. Essent. Oil Res. 32, 512–525. https://doi.org/10.1080/10412905.2020.1813212.

Kavoosi, G., Rowshan, V., 2013. Chemical composition, antioxidant and antimicrobial activities of essential oil obtained from *Ferula assa-foetida* oleo-gum-resin: effect of collection time. Food Chem. 138, 2180–2187. https://doi.org/10.1016/j.foodchem.2012.11.131.

Kirk, R.D., Akanji, T., Li, H., Shen, J., Allababidi, S., Seeram, N.P., Bertin, M.J., Ma, H., 2022. Evaluations of skin permeability of cannabidiol and its topical formulations by skin membrane-based parallel artificial membrane permeability assay and franz cell diffusion assay. Med. Cannabis Cannabinoids 5, 129–137. https://doi.org/10.1159/000526769.

Ksouda, G., Sellimi, S., Merlier, F., Falcimaigne-Cordin, A., Thomasset, B., Nasri, M., Hajji, M., 2019. Composition, antibacterial and antioxidant activities of *Pimpinella saxifraga* essential oil and application to cheese preservation as coating additive. Food Chem. 288, 47–56. https://doi.org/10.1016/j.foodchem.2019.02.103.

Labed-Zouad, I., Labed, A., Laggoune, S., Zahia, S., Kabouche, A., Kabouche, Z., 2015. Chemical compositions and antibacterial activity of four essential oils from *Ferula vesceritensis* Coss. & Dur. against clinical isolated and food-borne pathogens. Rec. Nat. Prod. 9, 518–525.

Lemouchi, R., Selles, C., Dib, M.E.A., Benmansour, N., Allal, A., Tabti, B., Ouali, K., 2017. Chemical composition and antioxidant activity of essential oil and hydrosol extract obtained by hydrodistillation (HY) and liquid–liquid extraction (LLE) of *Psoralea bituminosa*. J. Herbs Spices Med. Plants 23, 299–307. https://doi.org/10.1080/10496475.2017.1329765.

Liu, H., Ren, Z.L., Wang, W., Gong, J.X., Chu, M.J., Ma, Q.W., Wang, J.C., Lv, X.H., 2018. Novel coumarin-pyrazole carboxamide derivatives as potential topoisomerase II inhibitors: Design, synthesis and antibacterial activity. Eur. J. Med. Chem. 157, 81–87. https://doi.org/10.1016/j.ejmech.2018.07.059.

Liu, T., Wang, L., Zhang, L., Jiang, H., Zhang, Y., Mao, L., 2020b. Insecticidal, cytotoxic and anti-phytopathogenic fungal activities of chemical constituents from the aerial parts of *Ferula sinkiangensis*. Nat. Prod. Res. 34, 1430–1436. https://doi.org/10.1080/14786419.2018.1509328.

Liu, C., Xu, Y., Kirk, R.D., Li, H., Li, D., DaSilva, N.A., Bertin, M. J., Seeram, N.P., Ma, H., 2020a. Inhibitory effects of skin permeable glucitol-core containing gallotannins from red maple leaves on elastase and their protective effects on human keratinocytes. J. Funct. Foods 75,. https://doi.org/10.1016/j.jff.2020.104208 104208.

Lynch, B.J., Guinee Jr, D.G., Holden, J.A., 1997. Human DNA topoisomerase II-alpha: a new marker of cell proliferation in invasive breast cancer. Hum. Pathol. 28, 1180–1188. https://doi.org/10.1016/S0046-8177(97)90256-2.

Maggi, F., Cecchini, C., Cresci, A., Coman, M.M., Tirillini, B., Sagratini, G., Papa, F., 2009. Chemical composition and antimicrobial activity of the essential oil from *Ferula glauca* L. (*F. communis* L. subsp. glauca) growing in Marche (central Italy). Fitoterapia 80, 68–72. https://doi.org/10.1016/j.fitote.2008.10.001.

Mischko, W., Hirte, M., Fuchs, M., Mehlmer, N., Brück, T.B., 2018. Identification of sesquiterpene synthases from the Basidiomycota *Coniophora puteana* for the efficient and highly selective β-copaene and cubebol production in *E. coli*. Microb. Cell Factories 17, 164. https://doi.org/10.1186/s12934-018-1010-z.

Moghrovyan, A., Parseghyan, L., Sevoyan, G., Darbinyan, A., Sahakyan, N., Gaboyan, M., Voskanyan, A., 2022. Antinociceptive, anti-inflammatory, and cytotoxic properties of *Origanum vulgare* essential oil, rich with β-caryophyllene and β-caryophyllene oxide. Korean J. Pain 35, 140–151. https://doi.org/10.3344/kjp.2022.35.2.140.

Nafis, A., Kasrati, A., Jamali, C.A., Mezrioui, N., Setzer, W., Abbad, A., Hassani, L., 2019. Antioxidant activity and evidence for synergism of *Cannabis sativa* (L.) essential oil with antimicrobial standards. Ind. Crops Prod. 137, 396–400. https://doi.org/10.1016/j.indcrop.2019.05.032.

National Institute of Standards and Technology, NIST, 2014. NIST/EPA/NIH Mass Spectral Library, NIST Standard Reference Database Number 69. The NIST Mass Spectrometry Data Center, Gaithersburg, MD, USA.

Nguir, A., Mabrouk, H., Douki, W., Ismail, M.B., Ben Jannet, H., Flamini, G., 2016. Chemical composition and bioactivities of the essential oil from different organs of *Ferula communis* L. growing in Tunisia. Med. Chem. Res. 25, 515–525. https://doi.org/10.1007/s00044-016-1506-1.

Pavela, R., Morshedloo, M.R., Lupidi, G., Carolla, G., Barboni, L., Quassinti, L., Benelli, G., 2020. The volatile oils from the oleogum-resins of *Ferula assa-foetida* and *Ferula gummosa*: a comprehensive investigation of their insecticidal activity and eco-toxicological effects. Food Chem. Toxicol. 140,. https://doi.org/10.1016/j.fct.2020.111312 111312.

Pei, X.D., Yao, H.L., Shen, L.Q., Yang, Y., Lu, L., Xiao, J.S., Jiang, L.H., 2020. α-Cyperone inhibits the proliferation of human cervical cancer HeLa cells via ROS-mediated PI3K/Akt/mTOR signaling pathway. Eur. J. Pharmacol. 883,. https://doi.org/10.1016/j.ejphar.2020.173355 173355.

Radünz, M., da Trindade, M.L.M., Camargo, T.M., Radünz, A.L., Borges, C.D., Gandra, E.A., Helbig, E., 2019. Antimicrobial and antioxidant activity of unencapsulated and encapsulated clove (*Syzygium aromaticum*, L.) essential oil. Food Chem. 276, 180–186. https://doi.org/10.1016/j.foodchem.2018.09.173.

Ruch, R.J., Cheng, S.J., Klaunig, J.E., 1989. Prevention of cytotoxicity and inhibition of intercellular communication by antioxidant catechins isolated from Chinese green tea. Carcinogenesis 10, 1003–1008. https://doi.org/10.1093/carcin/10.6.1003.

Sabulal, B., Dan, M., Kurup, R., Pradeep, N.S., Valsamma, R.K., George, V., 2006. Caryophyllene-rich rhizome oil of *Zingiber nimmonii* from South India: Chemical characterization and antimicrobial activity. Phytochemistry 67, 2469–2473. https://doi.org/10.1016/j.phytochem.2006.08.003.

Saidi, I., Manachou, M., Znati, M., Bouajila, J., Ben Jannet, H., 2022. Synthesis of new halogenated flavonoid-based isoxazoles: *In vitro* and *in silico* evaluation of α-amylase inhibitory potential, a SAR analysis and DFT studies. J. Mol. Struct. 1247,. https://doi.org/10.1016/j.molstruc.2021.131379 131379.

Sarikurkcu, C., Ozer, M.S., Calli, N., Popović-Djordjević, J., 2018. Essential oil composition and antioxidant activity of endemic *Marrubium parviflorum* subsp. oligodon. Ind. Crops Prod. 119, 209–213. https://doi.org/10.1016/j.indcrop.2018.04.023.

Savelev, S., Okello, E., Perry, N.S.L., Wilkins, R.M., Perry, E.K., 2003. Synergistic and antagonistic interactions of anticholinesterase terpenoids in *Salvia lavandulaefolia* essential oil. Pharmacol. Biochem. Behav. 75, 661–668. https://doi.org/10.1016/S0091-3057(03)00125-4.

Schofs, L., Sparo, M.D., Sánchez Bruni, S.F., 2021. The antimicrobial effect behind *Cannabis sativa*. Pharmacol. Res. Perspect. 9, e00761. https://doi.org/10.1002/prp2.761.

Shahrajabian, M.H., Sun, W., Soleymani, A., Khoshkaram, M., Cheng, Q., 2021. Asafoetida, god's food, a natural medicine. Pharmacogn. Commun. 11. https://doi.org/10.5530/pc.2021.1.8.

Sharopov, F.S., Khalifaev, P.D., Satyal, P., Sun, Y., Safomuddin, A., Musozoda, S., Setzer, W.N., 2019. The chemical composition and biological activity of the essential oil from the underground parts of *Ferula tadshikorum* (Apiaceae). Rec. Nat. Prod. 13, 18–23. https://doi.org/10.25135/rnp.65.18.02.089.

Shatar, S., 2005. Essential oil of *Ferula ferulaoides* from Western Mongolia. Chem. Nat. Compd. 41, 607–608. https://doi.org/10.1007/s10600-005-0222-8.

Silva, A.M.A., da Silva, H.C., Monteiro, A.O., Lemos, T.L.G., de Souza, S.M., Militão, G.C.G., Santiago, G.M.P., 2020. Chemical composition, larvicidal and cytotoxic activities of the leaf essential oil of *Bauhinia cheilantha* (Bong.) Steud. S. Afr. J. Bot. 131, 369–373. https://doi.org/10.1016/j.sajb.2020.03.011.

Sonigra, P., Meena, M., 2021. Metabolic profile, bioactivities, and variations in the chemical constituents of essential oils of the *Ferula* genus (Apiaceae). Front. Pharmacol. 11,. https://doi.org/10.3389/fphar.2020.608649 608649.

Srivastava, R., 2021. Theoretical studies on the molecular properties, toxicity, and biological efficacy of 21 new chemical entities. ACS Omega 6, 24891–24901. https://doi.org/10.1021/acsomega.1c03736.

Su, Y.C., Ho, C.L., 2016. Composition of the leaf essential oil of *Phoebe formosana* from Taiwan and its *in vitro* cytotoxic, antibacterial, and antifungal activities. Nat. Prod. Commun. 11, 845–848. https://doi.org/10.1177/1934578X1601100637.

Sylvestre, M., Legault, J., Dufour, D., Pichette, A., 2005. Chemical composition and anticancer activity of leaf essential oil of *Myrica gale* L. Phytomedicine 12, 299–304. https://doi.org/10.1016/j.phymed.2003.12.004.

Tian, H., Zhao, H., Zhou, H., Zhang, Y., 2019. Chemical composition and antimicrobial activity of the essential oil from the aerial part of *Dictamnus dasycarpus* Turcz. Ind. Crops Prod. 140,. https://doi.org/10.1016/j.indcrop.2019.111713 111713.

Toan, D.N., Thanh, N.D., Truong, M.X., Van, D.T., 2020. Quinoline-pyrimidine hybrid compounds from 3-acetyl-4-hydroxy-1-methylquinolin-2(1*H*)-one: study on synthesis, cytotoxicity, ADMET and molecular docking. Arab. J. Chem. 13, 7860–7874. https://doi.org/10.1016/j.arabjc.2020.09.018.

Topdas, E.F., Sengul, M., Taghizadehghalehjoughi, A., Hacimuftuoglu, A., 2020. Neuroprotective potential and antioxidant activity of various solvent extracts and essential oil of *Ferula orientalis* L. J. Essent. Oil-Bear. Plants 23, 121–138. https://doi.org/10.1080/0972060X.2020.1729247.

Tripathi, A.K., Rawat, S., Mitra, S., Sharma, U., Sharma, K., 2019. A review on pharmacological actions of *Ferula asafoetida* oleo-gum-resin (hingu) in the management of abdominal pain. Curr. Med. Drug Res. 3, 192.

Trott, O., Olson, A.J., 2010. AutoDock Vina: improving the speed and accuracy of docking with a new scoring function, efficient optimization, and multithreading. J. Comput. Chem. 31, 455–461. https://doi.org/10.1002/jcc.21334.

Tuncay, H.O., Olcay, B., Uruşak, E.A., 2019. Comparative morphology and fruit anatomy of *Ferula szowitsiana* DC. and *Ferula caspica* M. Bieb. J. Res. Pharm. 23, 577–583. https://doi.org/10.12991/jrp.2019.165.

Ullah, H., Di Minno, A., Santarcangelo, C., Khan, H., Daglia, M., 2021. Improvement of oxidative stress and mitochondrial dysfunction by β-caryophyllene: a focus on the nervous system. Antioxidants 10 (4), 546. https://doi.org/10.3390/antiox10040546.

Wan Salleh, W.M.N.H., Kammil, M.F., Ahmad, F., Sirat, H.M., 2015. Antioxidant and anti-inflammatory activities of essential oil and extracts of *Piper miniatum*. Nat. Prod. Commun. 10, 2005–2008. https://doi.org/10.1177/1934578X1501001151.

Wang, G.H., Ahmed, A.F., Sheu, J.H., Duh, C.Y., Shen, Y.C., Wang, L.T., 2002. Suberosols A-D, four new sesquiterpenes with β-caryophyllene skeletons from a Taiwanese gorgonian coral *Subergorgia suberosa*. J. Nat. Prod. 65, 887–891. https://doi.org/10.1021/np010586i.

Yakhlef, G., Hambaba, L., Pinto, D.C., Silva, A.M., 2020. Chemical composition and insecticidal, repellent and antifungal activities of essential oil of *Mentha rotundifolia* (L.) from Algeria. Ind. Crops Prod. 158,. https://doi.org/10.1016/j.indcrop.2020.112988 112988.

Ye, Z., Yang, Y., Li, X., Cao, D., Ouyang, D., 2018. An integrated transfer learning and multitask learning approach for pharmacokinetic parameter prediction. Mol. Pharm. 16, 533–541. https://doi.org/10.1021/acs.molpharmaceut.8b00816.

Zafar, F., Gupta, A., Thangavel, K., Khatana, K., Sani, A.A., Ghosal, A., Tandon, P., Nishat, N., 2020. Physicochemical and pharmacokinetic analysis of anacardic acid derivatives. ACS Omega 5, 6021–6030. https://doi.org/10.1021/acsomega.9b04398.

Zardi-Bergaoui, A., Jelizi, S., Flamini, G., Ascrizzi, R., Ben Jannet, H., 2018. Comparative study of the chemical composition and bioactivities of essential oils of fresh and dry seeds from *Myoporum insulare* R. Br. Ind. Crops Prod. 111, 232–237. https://doi.org/10.1016/j.indcrop.2017.10.019.

Zardi-Bergaoui, A., Znati, M., Harzallah-Skhiri, F., Ben Jannet, H., 2019. Caryophyllene sesquiterpenes from *Pulicaria vulgaris* Gaertn.: isolation, structure determination, bioactivity and structure–activity relationship. Chem. Biodivers. 16, e1800483.

Zardi-Bergaoui, A., Jelassi, A., Daami-Remadi, M., Harzallah-Skhiri, F., Flamini, G., Ascrizzi, R., Ben Jannet, H., 2020. Chemical composition and bioactivities of essential oils from *Pulicaria vulgaris* subsp. *dentata* (Sm.) Batt. growing in Tunisia. J. Essent. Oil Res. 32, 111–120. https://doi.org/10.1080/10412905.2019.1698468.

Zengin, G., Sinan, K.I., Ak, G., Mahomoodally, M.F., Paksoy, M. Y., Picot-Allain, C., Custodio, L., 2020. Chemical profile, antioxidant, antimicrobial, enzyme inhibitory, and cytotoxicity of seven Apiaceae species from Turkey: a comparative study. Ind. Crops Prod. 153,. https://doi.org/10.1016/j.indcrop.2020.112572 112572.

Zhou, J., Wei, J., Liu, Z., 2020. An expanded circumscription for the previously monotypic *Pleurospermopsis* (Apiaceae) based on nrDNA ITS sequences and morphological evidence. Phytotaxa 460, 129–136. https://doi.org/10.11646/phytotaxa.460.2.2.

Znati, M., Jabrane, A., Hajlaoui, H., Harzallah-Skhiri, F., Bouajila, J., Casanova, J., Ben Jannet, H., 2012. Chemical composition and *in vitro* evaluation of antimicrobial and anti-acetylcholinesterase properties of the flower oil of *Ferula lutea*. Nat. Prod. Commun. 7, 947–950. https://doi.org/10.1177/1934578X1200700738.

Znati, M., Filali, I., Jabrane, A., Casanova, J., Bouajila, J., Ben Jannet, H., 2017. Chemical composition and *in vitro* evaluation of antimicrobial, antioxidant and antigerminative properties of the seed oil from the Tunisian endemic *Ferula tunetana* Pomel ex Batt. Chem. Biodivers. 14, e1600116.

Znati, M., Bordes, C., Forquet, V., Lanteri, P., Ben Jannet, H., Bouajila, J., 2019. Synthesis, molecular properties, anti-inflammatory and anticancer activities of novel 3-hydroxyflavone derivatives. Bioorg. Chem. 89,. https://doi.org/10.1016/j.bioorg.2019.103009 103009.